The Canadian Mineralogist
Vol. 31, pp. 997-1024 (1993)

MINERALOGY AND GEOCHEMISTRY OF ACTIVE AND INACTIVE CHIMNEYS AND MASSIVE SULFIDE, MIDDLE VALLEY, NORTHERN JUAN DE FUCA RIDGE: AN EVOLVING HYDROTHERMAL SYSTEM*

DOREEN E. AMES, JAMES M. FRANKLIN AND MARK D. HANNINGTON

Geological Survey of Canada, 601 Booth Street, Ottawa, Ontario K1A 0E8

ABSTRACT

Hydrothermal deposits occur at a water depth of 2460 m in Middle Valley, a sediment-filled failed rift at 48°27′ N latitude, on the northern Juan de Fuca Ridge. Sites of focused discharge are concentrated above a deep-seated system of fractures parallel to the regional north–south trend of rift-propagating faults. The Area of Active Venting (AAV) and Bent Hill area are hosts to moderate-temperature (<276°C) vents. Active chimneys are sulfate-rich and sulfide-poor, consisting of a thick outer wall of anhydrite and a thin clay-rich inner wall with very fine (20 μm) disseminated sulfides. The inner wall contains saponite, pyrrhotite, chalcopyrite, isocubanite, high-iron sphalerite (35–46 mole % FeS), pyrite, marcasite, galena and arsenopyrite. The active chimneys have low concentrations of the base metals but a high Cu/Zn value. The fluids discharging through these chimneys have characteristically low $a(O_2)$ and $a(S_2)$, and locally have deposited significant amounts of hydrocarbon. Hydrothermal mounds associated with active venting are produced by the collapse of chimneys and by mineral precipitation within the pile of sulfide–sulfate talus (*i.e.*, by inflation). The active mounds are composed of anhydrite, amorphous silica, saponite, serpentine, and minor chalcopyrite, low-iron sphalerite (<15 mole % FeS), lepidocrocite, pyrite, marcasite, galena and barite. Inactive chimneys on or adjacent to the mounds are predominantly barite-rich, with lesser amorphous silica, hydrocarbons, clay and marcasite. In contrast to the active chimneys, the Bent Hill deposits are sulfide-rich and have higher Zn/Cu values. Two older massive sulfide deposits in the Bent Hill area contain pyrite, lepidocrocite, marcasite, moderately iron-rich sphalerite (24–33 mole % FeS), chalcopyrite, covellite, galena, silica and barite. Pb–As–Sb sulfosalts occur locally within low-temperature, silica-rich crusts on the massive sulfides. The mineralogy and geochemistry of the active chimneys suggest that the present stage of hydrothermal venting at Middle Valley is both metal- and sulfur-depleted and is likely the product of the moderate-temperature interaction of hydrothermally modified seawater with local sediments. The massive sulfides at Bent Hill are apparently a product of an earlier hydrothermal event dominated by metal- and sulfur-enriched fluids, possibly derived from the high-temperature interaction of circulating seawater with basaltic crust in the basement. Recent drilling by the ODP has identified a large pyrite – pyrrhotite – magnetite deposit beneath the sulfide outcrop at Bent Hill. The present-day mineralogy of this older massive sulfide deposit may be the product of extensive reaction with the cool, sulfur-depleted fluids that are currently venting at Middle Valley.

Keywords: massive sulfide, Middle Valley, Juan de Fuca Ridge, chemical composition, mineralogy, mineral chemistry, seafloor, hydrothermal, anhydrite.

SOMMAIRE

Nous documentons la présence de zones d'activité hydrothermale à une profondeur de 2,460 m le long de Middle Valley, rift avorté rempli de sédiments à une latitude de 48°27′N, dans la partie nord de la ride de Juan de Fuca. Les sites de décharge focalisée sont surtout situés au dessus d'une zone de fractures profondes, parallèle à la direction régionale des failles servant à propager la distension. Deux zones, dites "Area of Active Venting" et "Bent Hill", sont les sites d'évents à température moyenne (<276°C). Les cheminées actives sont riches en sulfates et pauvres en sulfures, et sont faites d'une épaisse paroi externe d'anhydrite et d'une mince paroi interne riche en argiles, contenant des sulfures disséminés à granulométrie très fine (20 μm). La paroi interne contient saponite, pyrrhotite, chalcopyrite, isocubanite, sphalérite à teneur élevée en fer (35–46% de FeS, base molaire), pyrite, marcasite, galène et arsenopyrite. Les cheminées actives font preuve de faibles teneurs en métaux de base et d'un rapport Cu/Zn élevé. La phase fluide déchargée de ces cheminées, typiquement à $a(O_2)$ et $a(S_2)$ faibles, aurait localement produit des quantités appréciables d'hydrocarbures. Les amoncellements hydrothermaux associés aux zones d'activité résultent de l'affaissement des cheminées et de la précipitation de minéraux à l'intérieur des talus de sulfure – sulfate (c'est-à-dire, par inflation). Les amoncellements actifs contiennent anhydrite, silice amorphe, saponite, et serpentine, avec, comme accessoires, chalcopyrite, sphalérite à faible teneur en fer (<15% FeS), lépidocrocite, pyrite, marcasite, galène et barite. Les cheminées inactives sur ou près de ces amoncellements contiennent surtout de la barite, avec des quantités moindres de silice amorphe, d'hydrocarbures, d'argiles et de marcasite. En contraste avec les cheminées actives, les gisements de Bent

* Geological Survey of Canada contribution number 42592.

Hill sont riches en sulfures, et possèdent un rapport Zn/Cu plus élevé. Deux gîtes plus anciens près de Bent Hill contiennent pyrite, lépidocrocite, marcasite, sphalérite à teneur moyenne en fer (24–33% FeS), chalcopyrite, covellite, galène, silice et barite. Nous avons trouvé des sulfosels à Pb–As–Sb dans des incrustations siliceuses formées sur les sulfures massifs à faible température. La minéralogie et la géochimie des cheminées actives font penser que le stade actuel d'activité hydrothermale à Middle Valley est à la fois pauvre en métaux et en soufre, et résulterait de l'interaction à température moyenne de l'eau de mer modifiée et des sédiments enfouis. Les sulfures massifs de Bent Hill résulteraient d'un événement antérieur, où prédominaient des fluides enrichis en métaux et en sulfures, possiblement dérivés de l'interaction à température élevée de l'eau de mer en circulation et de la croûte basaltique du socle. Des forages récents (programme ODP) ont permis d'identifier un gisement important à pyrite + pyrrhotite + magnétite en dessous de l'affleurement de sulfures à Bent Hill. L'assemblage minéralogique actuel de ce gisement ancien de sulfures massifs pourrait bien être le résultat d'une réaction importante avec les fluides appauvris en soufre et plus froids qui émanent présentement des évents à Middle Valley.

(Traduit par la Rédaction)

Mots-clés: sulfures massifs, Middle Valley, ride de Juan de Fuca, composition chimique, minéralogie, composition des minéraux, fonds océaniques, hydrothermal, anhydrite.

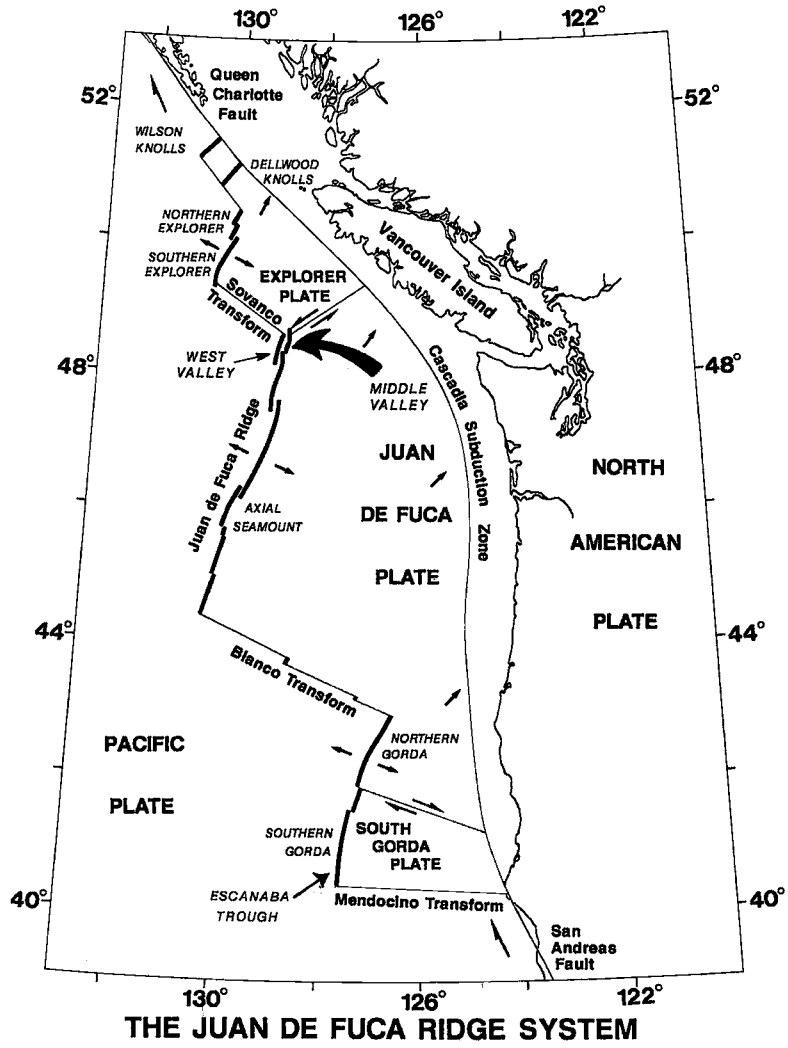

FIG. 1. Location map of Middle Valley, northern Juan de Fuca Ridge.

INTRODUCTION

Much of the recent research on massive sulfide deposits on the modern seafloor has been restricted to sediment-starved ridges in the eastern Pacific and mid-Atlantic. However, the first discovery of active deposition of base metals on the seafloor was made in sediment-covered basins in the Red Sea, a continental rift (Degens & Ross 1969). The importance of massive sulfide deposits in a sediment-covered oceanic spread-

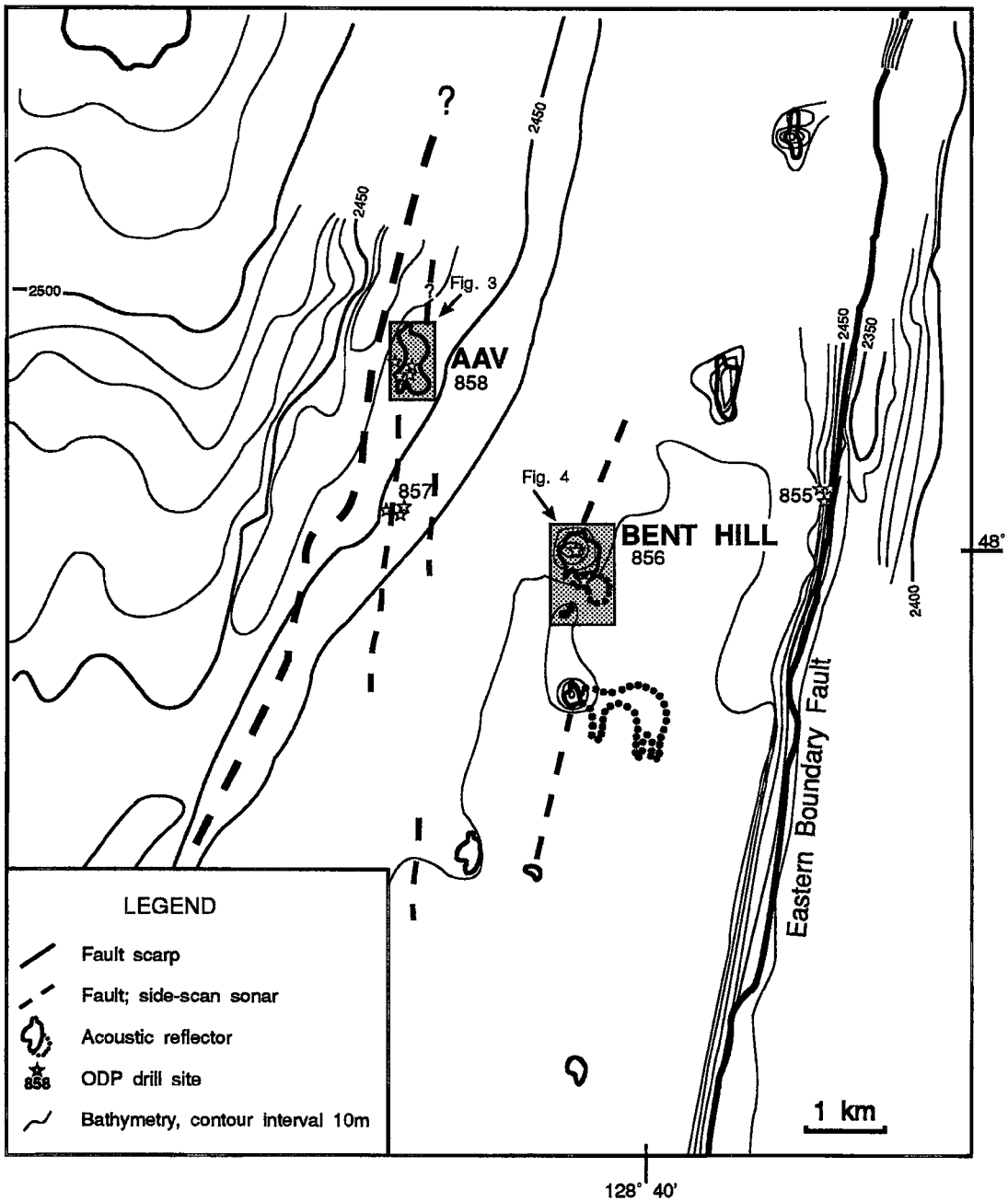

FIG. 2. Location of the Area of Active Venting (AAV) and Bent Hill hydrothermal areas, situated west of the eastern boundary fault within Middle Valley. Fault traces and ODP drill sites are shown. The diagram was compiled from bathymetric data from Currie *et al.* (1985), with acoustic reflectors and fault traces superimposed [from SeaMARC 1A imagery: Franklin *et al.* (in press) and SeaMARC II imagery: Davis *et al.* (1992)]. Locations of Figures 3 and 4 are indicated.

ing axis was realized with the discovery of sulfide mineralization in the Guaymas Basin, Gulf of California (Lonsdale *et al.* 1980).

Mapping of mid-ocean ridges off the western continental margin of North America has revealed a number of sediment-covered basins filled with turbiditic material shed off the adjacent continental margin. Investigations of sediment-covered rifts along the northern Juan de Fuca and southern Gorda Ridge segments led to the discovery of sulfide deposits, at Escanaba Trough (Morton *et al.* 1987) and at Middle Valley (Davis *et al.* 1987) (Fig. 1). The recovery of sulfide samples in dredges and sediment cores from Middle Valley prompted an ALVIN dive series in 1990 (Franklin *et al.* 1991) during which scientists observed, photographed, and collected actively discharging chimneys. Samples of moderate-temperature (184 to 276°C) vent fluids, sulfide and sulfate chimneys, massive sulfide, hydrothermally altered and unaltered sediment, and vent-specific benthic fauna were recovered.

This contribution documents the composition of the surficial massive sulfide deposits, hydrothermal mounds, inactive and active chimneys, and barite-rich crusts at Middle Valley and considers their relationship to the evolution of the hydrothermal system. These results are compared with data from hydrothermal sites on other sedimented ridges and with the results of recent drilling by the ODP beneath the active vents at Middle Valley. The investigation of sediment-hosted volcanogenic massive sulfide deposits is important in that many of the world's largest massive sulfide deposits are hosted either at the contact between volcanic and sedimentary sequences

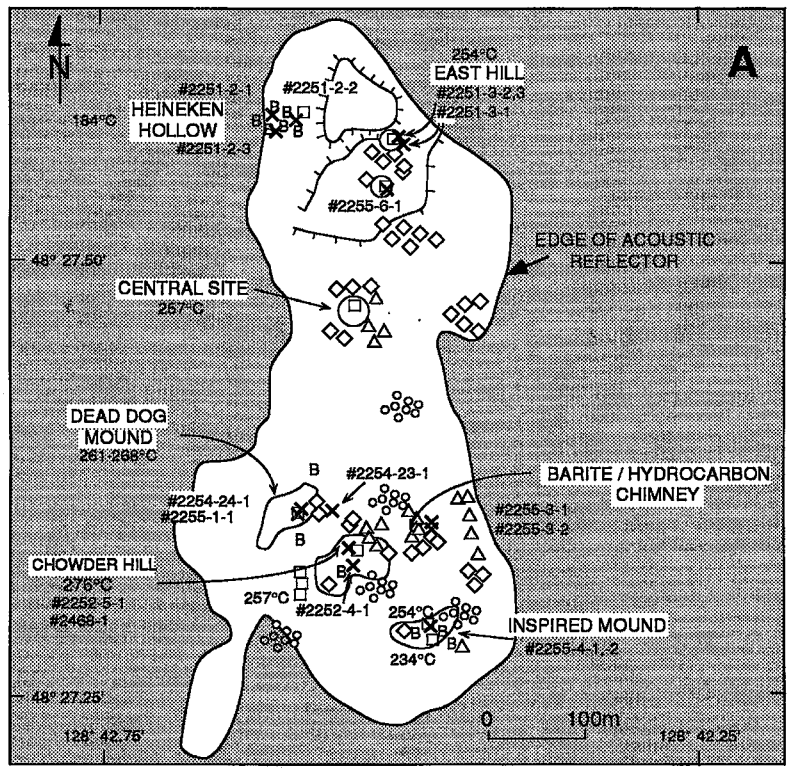

FIG. 3A. Detailed geological map of the Area of Active Venting (AAV), with location of rock samples studied.

or within the sedimentary basin-fill in a volcanically active terrane.

Geology and Hydrothermal Activity at Middle Valley

Middle Valley is a 15-km-wide, sediment-covered axial rift within the Juan de Fuca Ridge system; it is located 200 km off the coast of Vancouver Island (Fig. 1). Two sediment-covered spreading centers with active hydrothermal systems on the Juan de Fuca Ridge include Middle Valley and Escanaba Trough (Fig. 1), both sites of sulfide deposition.

Middle Valley was recently an active mid-ocean spreading center until approximately 200,000 years ago, when spreading jumped west to the now-active, sediment-buried, intermediate-rate spreading center in West Valley (60 mm/yr) (Davis & Lister 1977). Middle Valley is still undergoing minor readjustment, as indicated by the presence of fissures and faults within the sediment fill in the valley, which controls the position of the present-day hydrothermal activity (Fig. 2). Seismic profiles across the valley indicate a series of downstepping block-faults, with the deepest part of the valley along the axis. The surface expression of the faults indicates that most are parallel to the regional north–south trend of the rift-propagating regional faults, but several oblique NW–SE structures also are present (Johnson *et al.* 1990).

Middle Valley is filled with turbiditic and hemipelagic sediment derived from the continental margin during the Pleistocene, dominantly from Queen Charlotte Sound. Two known sites of hydrothermal activity, the Area of Active Venting

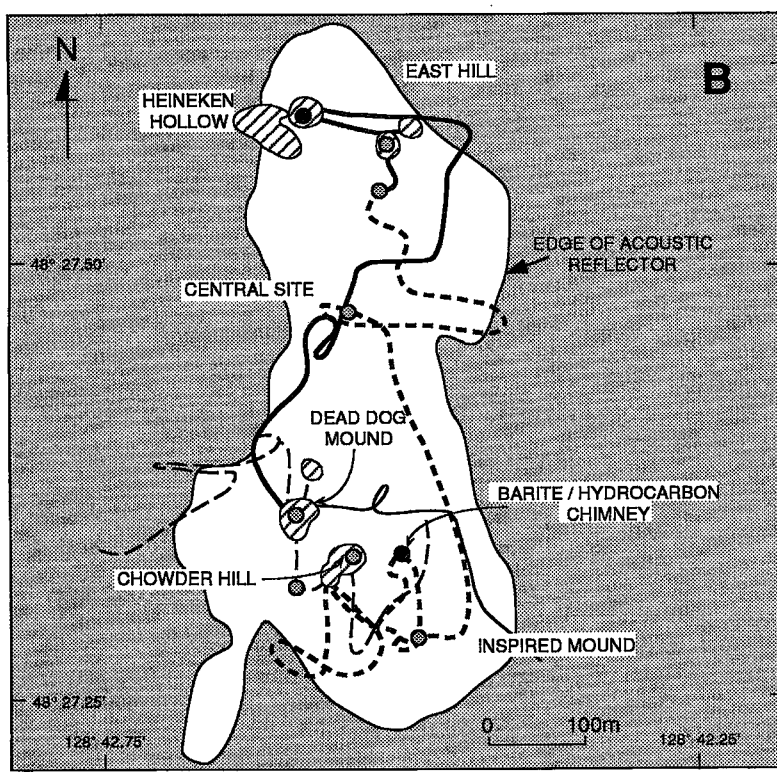

FIG. 3B. Dive tracks 2251, 2252, 2254, 2255 of the ALVIN submersible in the Area of Active Venting, showing the extent of exploration.

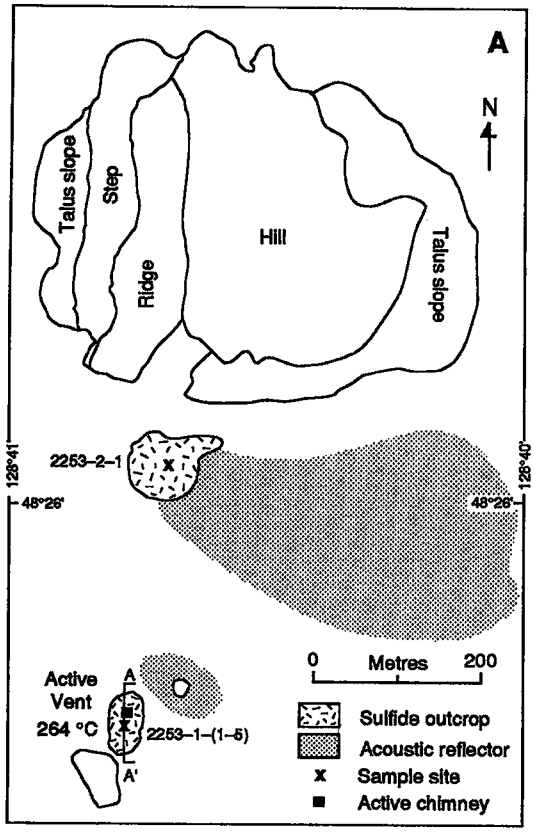

FIG. 4A. Geology of the Bent Hill area, with acoustically reflectant areas outlining known massive sulfide deposits. Location of rock samples studied is shown. A–A': location of cross-section.

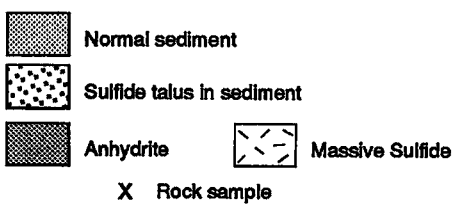

FIG. 4B. Cross section from A to A' and detailed plan-view of the Bent Hill active chimney and associated sulfide mound. The samples used in this study are indicated.

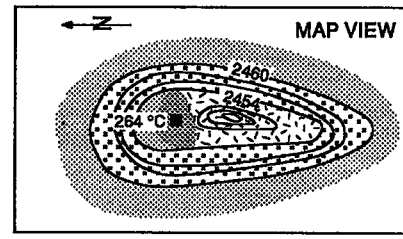

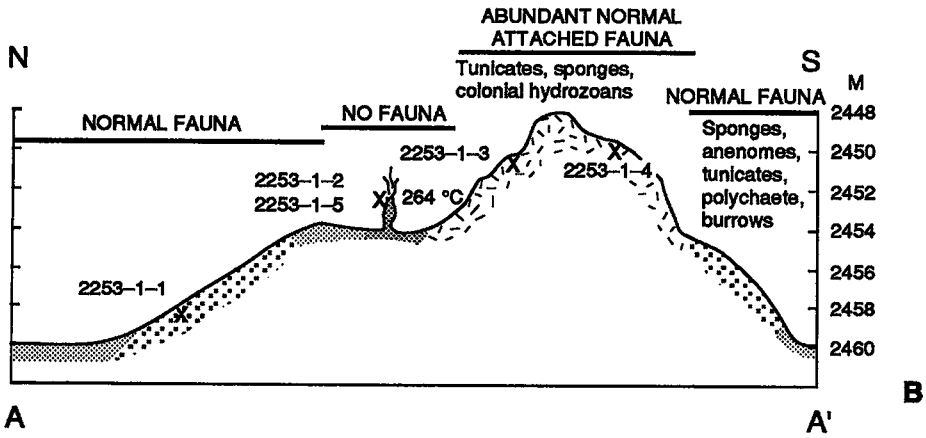

(AAV) and Bent Hill, are situated on the eastern side of the valley 5 km and 3 km west of the eastern boundary fault, respectively, at a water depth of 2460 m (Fig. 2). The two sites of active hydrothermal venting were identified from geological (Franklin *et al.* 1987) and geophysical (Davis *et al.* 1987) observations. The more northerly, Area of Active Venting (AAV), is defined by anomalously high acoustic reflectance (Figs. 2, 3), and has over 20 vent sites. The zones of high reflectance represent aprons of hydrothermally indurated sediment surrounding the vent sites (Franklin *et al.* 1991). Another zone of high reflectance, south of Bent Hill (Fig. 2), is a prominent mound of sulfide, with a single moderate-temperature (264°C) vent. A very large pyritic massive sulfide deposit (at least 150 × 150 × 96 m) has been documented (Davis *et al.* 1992) about 100 m south of Bent Hill and 230 m north of the active vent (Figs. 2, 4).

Drilling and seismic data reveal that Middle Valley contains over 1000 m of turbiditic and hemipelagic sediment, and a variety of intrusive and extrusive rocks. The sediments are well lithified at a depth of 400 m in the center of the basin, and at a depth of 175 m below the AAV (see velocity – density – porosity data: Davis *et al.* 1992). The composition of the basement at Middle Valley is unknown, but ODP drilling intersected a variety of sills and extrusive rocks, including normal MORB-type basalt at the basin margins along the eastern boundary fault (site 855, Fig. 2), about 30 basaltic sills below 500 mbsf near the center of the valley (site 857, Fig. 2) and "evolved" andesitic basalt 250 mbsf under the AAV (site 858, Fig. 2). The volcanic rocks beneath the AAV form a paleobathymetric high, possibly a seamount or a structurally uplifted block. On Bent Hill, turbiditic sediment-fill exceeds 960 mbsf, and a series of young, relatively fresh picritic sills has intruded the sediment to a depth of only 60 mbsf (Stakes *et al.* 1991).

Area of Active Venting

The AAV is an area of anomalously high heat-flow (*i.e.*, >1 W m^{-2}: Davis *et al.* 1987) and is the site of at least 20 active vents with moderate temperatures between 184° and 276°C (Franklin *et al.* 1991). The vent field is 800 m by 350 m, roughly rhombohedral and elongate along a north–south axis (Fig. 3). Traces of faults (Fig. 2), evident on side-scan sonar maps, extend away from the southwestern and northeastern corners of the acoustic reflector. Both faults are longitudinal, and probably correspond to a major buried fault that is evident in seismic profiles (Davis *et al.* 1992).

The AAV is characterized by active chimneys with anhydrite, inactive chimneys with barite, hydrothermal mounds, and chimney rubble, but lacks any surface expression of massive sulfide (Fig. 3A). Numerous inactive barite-rich chimneys were found throughout the AAV. Distinctive topographic highs within the AAV are low hydrothermal mounds with active and inactive chimneys, 1 to 6 m high, located near their summits. The area of high acoustic reflectance contains two groups of mounds. The northern group includes Heineken Hollow, East Hill, and Central Site, and the southern group includes Dead Dog Mound, Chowder Hill, and Inspired Mounds (Fig. 3A). Dead Dog Mound is representative of the mound and chimney morphology of active vents in Middle Valley (Figs. 3, 5A, B). The mound is 10 to 15 m high by 20 to 30 m wide, with steep sides sloping at about 30°. A 5- to 6-m-high conical chimney structure is perched on top of the mound, and vents hydrothermal fluids at 276°C. Blocks of chimney debris, 3–20 cm wide, form an apron several meters wide around the active vents. The sides of the mounds have many large displaced slabs of indurated sediment, typically 1 to 7 m wide, that attest to inflation of the hydrothermal mound. An extensive zone 2 to 3 m in diameter of white anhydrite envelops the base of the chimney, with local patches of bacterial mats on the surrounding mound. Dead tube-worms are attached to the base of the chimney, but otherwise the top of the mound is devoid of fauna. Numerous crabs inhabit the flanks of the mound, and small clusters of tube worms and clams live at its base. Vent communities are very dispersed, but the large clusters of tube worms that typify other ridge-crest vent areas are only poorly represented near the Middle Valley vents. Most chimneys observed during the 1990 dive series are similar in size and overall sulfide abundance to the Dead Dog site; however, the chimney sampled at Chowder Hill in 1991 (dive 2468) is about twice as large, contains more sulfide, and is perched on a mound 50 m wide by 15 m high.

Flow from the active vents throughout the AAV is vigorous; clear fluid and, in some cases, grey "smoke" emanate from the tops, and less well-focused clear fluid is discharging around the base of most chimneys. The vent-fluid temperatures range from 184° to 276°C. They have a pH of 5.3, high Ca and CO_2 contents and low contents of base metals in comparison with typical ridge-crest hydrothermal fluids (Von Damm & Bischoff 1987).

Inactive, barite-bearing chimneys are not located on mounds, are not specifically close to active vents, and sit on a flat, moderately indurated substrate. They are "rootless" in that they are underlain by sediment (Figs. 5C, D). At Heineken Hollow, barite crusts impregnated with silica, biological matter and altered sediment (Figs. 5E, F) surround a 3-m-deep collapsed pit. A low-temperature active vent occurs in the center of the pit.

Bent Hill

Bent Hill is one of several mounds projecting from the sediment-covered floor of Middle Valley. It is an

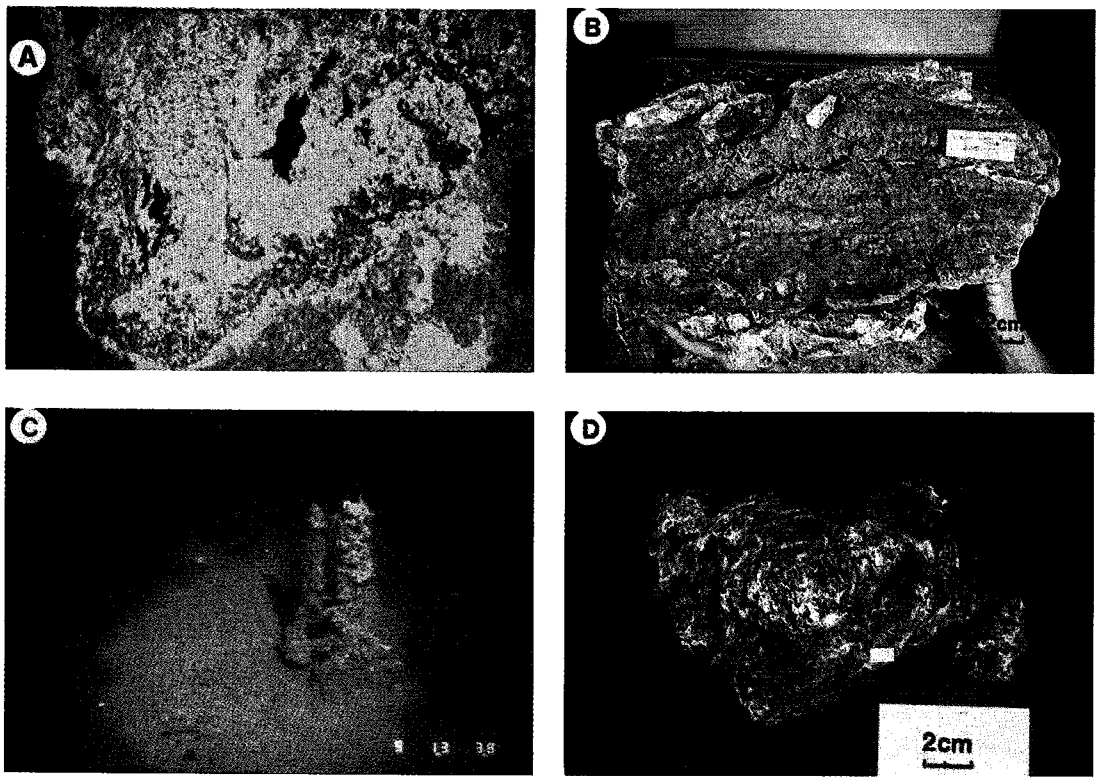

FIGS. 5A–D. A. Actively venting anhydrite chimneys on the top of a mound in the AAV. The chimneys are approximately 1 m high. B. Plan view of the central orifice of the Dead Dog mound active chimney. The top of the chimney is to the right. Note the white anhydrite outer zone (upper left and bottom) and the inner (dark grey) sulfide – Mg-bearing smectite lining. Scale card is 6.5 cm. C. Rootless inactive barite–bitumen chimney on the flat sediment seafloor in the Area of Active Venting. D. Cross-section of the top of a inactive chimney. Note the black bitumen and the semicircular pattern of growth of the brown barite.

uplifted block, approximately circular, 450 m in diameter and 60 m high, composed of turbiditic sediment and minor sulfide mud, sand and massive sulfide along the southern flank (Kappel & Franklin 1989, Joides 1991). Its western margin is very steep, covered by talus blocks composed of indurated sediment, and is probably a fault (Fig. 4A). Several picritic sills were intersected in ODP hole 856A and B; the uplift of Bent Hill may have occurred during their intrusion. Erosion of part of the sedimentary section, and the freshness of the talus blocks, indicate that uplift has postdated most of the sedimentation in the area, as well as the time of formation of a sulfide deposit to the south (ODP site 856C–H) (Davis *et al.* 1992).

In the Bent Hill area, one active chimney only was observed, but several extensive massive sulfide outcrops are present (Fig. 4A). Massive sulfide mineralization is observed at two sites 230 m apart. A sulfide outcrop at the base of Bent Hill (ODP site 856, Fig. 4A), was found through extensive camera and video studies, ALVIN observations, and piston coring; it is visible on side-scan sonar images (Franklin *et al.* 1987, 1991, Joides 1991). The sulfide deposit forms a distinct hill 35 m high and has a drill-indicated thickness of at least 96 m. This 100-m-long exposure is considered to be part of a more extensive sediment-covered deposit of sulfide possibly up to 250 × 450 m in plan view, as shown by the acoustic reflection outline (Fig. 4A).

The only known actively venting chimney at Bent Hill (264°C) is associated with a second sulfide deposit 230 m south of the ODP drilling site (856, Figs. 2, 4A, B, 5G, H). The active chimney is perched on the lower tier of a two-tiered mound structure, at an elevation of 15 m (Fig. 4B), with the highest tier at 28 m composed of sulfide outcrop and sulfide talus. The chimney is surrounded by an anhydrite apron and is quite similar morphologically to the active chimney

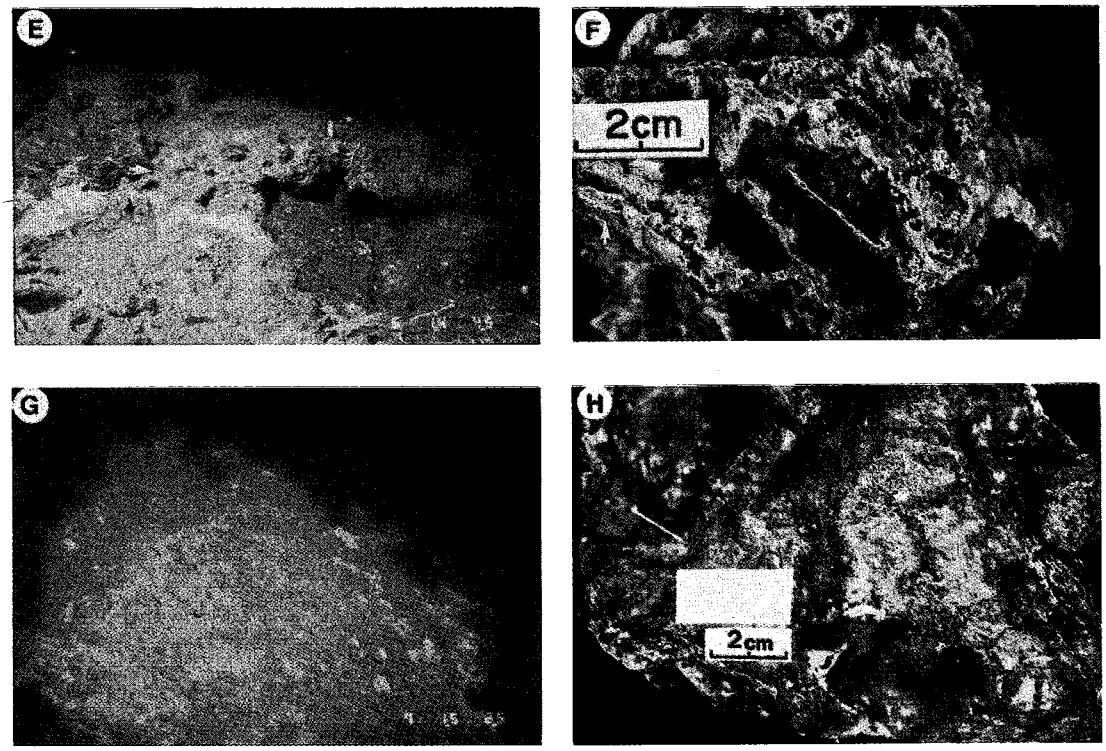

FIGS. 5E–H. E. Clear 184°C fluid venting from the depression at Heineken Hollow. Note the shimmering water at arrow. White anhydrite crusts and bacterial mats are near the vent, and barite-rich crusts are broken into slabs. F. Barite-rich crust at Heineken Hollow is very porous, with yellowish brown barite crystals as open-space fillings. Grey silica veinlets cross-cut the sample (arrow). G. Sulfide mound south of the Bent Hill active chimney. Note the angular blocks of sulfide and the oxidation effects on the outer margin of the outcrop. H. Porous massive sulfide talus from Bent Hill (2253–1–1, Fig. 3B) composed dominantly of pyrite, marcasite, sphalerite and chalcopyrite, with an outer oxidized rim.

sites at the AAV. Extensive weathering of the sulfide outcrop, the composition of the hydrothermal fluid (deduced by mineral assemblages, discussed below), and the large size of the Bent Hill sulfide deposit suggest that it may be significantly older than the surficial hydrothermal deposits in the AAV and the active vent at Bent Hill.

SAMPLING AND ANALYTICAL METHODS

The samples described in this paper were collected during a series of ALVIN dives (2251–2255) in 1990 and a subsequent dive (2468) in 1991. Sample locations are shown on Figures 3A and 4B, and those studied are listed in Table 1. Exploration of the AAV was much more extensive (five ALVIN dives; Fig. 3B) than in the Bent Hill area (ALVIN dive 2253). The hydrothermal material collected by the mechanical arm of ALVIN was subsampled and vacuum-impregnated with "petro epoxy". Sixty-one polished thin sections were prepared for petrographic examination by reflected and transmitted light. A Cambridge S–200 scanning electron microscope with a Link Analytical AN10000 integrated energy-dispersion X-ray analyzer attachment was used for identification of fine-grained (<2–20 μm) minerals. Quantitative mineral analyses were obtained with a Cameca Camebax wavelength-dispersion electron microprobe. The accelerating voltage was 20 kV, with a beam current of 30 nA and a beam-spot diameter of 5 μm. Bulk compositions were determined on air dried samples ground to –200 mesh. The powders were analyzed at the Geological Survey of Canada laboratories by inductively coupled plasma (ICP–ES), atomic absorption spectrometry (AAS), combustion and wet-chemical methods. Gold was determined by instrumental neutron-activation analysis (INAA) utilizing the facilities at the Royal Military College, Kingston,

TABLE 1. SAMPLE LIST AND SITE LOCATIONS FROM MIDDLE VALLEY

AREA OF ACTIVE VENTING			
ACTIVE CHIMNEY		INACTIVE CHIMNEY	
Sample	Site	Sample	Site
2251-1-1	DDM	2254-23-1	east of DDM
2251-2-2	HH	2255-3-2	IM
2251-2-3a	HH	2255-6-1	south of EH
2251-3-2	EH		
2251-3-3	EH	HYDROTHERMAL MOUND	
2255-3-1	east of DDM	Sample	Site
2255-4-1	IM		
2255-4-2	IM	2252-4-1B	CH
2468-1	CH	2252-4-1C	CH
		2252-5-1C	CH
		2254-24-1	DDM
BARITE CRUST			
Sample	Site		
2251-2-1	HH		
2251-2-3	HH		
BENT HILL AREA			
ACTIVE CHIMNEY		MASSIVE SULFIDE	
Sample	Site	Sample	Site
2253-1-2	SOUTH	2253-1-1	SOUTH
		2253-1-3	SOUTH
		2253-1-4	SOUTH
		2253-1-5	SOUTH
		2253-2-1	ODP 856

DDM=Dead Dog Mound, HH=Heineken Hollow, EH=East Hill, two separate chimneys, IM=Inspired Mounds, two separate chimneys, CH=Chowder Hill, SOUTH=see Figs.4A,B

Ontario, following the procedures outlined by Hannington & Gorton (1991).

Mineralogy and Paragenesis

Surficial deposits sampled by ALVIN at Middle Valley include active anhydrite-dominant chimneys, extinct barite- and hydrocarbon-bearing chimneys, barite-rich crusts, sulfide talus in sediment and massive sulfide outcrop. Samples studied are listed in Table 1, with their mineral assemblages summarized in Table 2, and textural characteristics are illustrated in Figures 5–9.

TABLE 2. MINERALOGY OF MIDDLE VALLEY HYDROTHERMAL SAMPLES

MINERAL	ACTIVE CHIMNEY	INACTIVE CHIMNEY	BARITE CRUST	MOUND	SULPHIDE DEPOSIT
anhydrite	A	-	-	-	-
gypsum	m	-	-	m	-
pyrrhotite	m	-	-	-	m
pyrite	tr	-	m	tr	A
marcasite	-	-	m	-	M
sphalerite	tr to m	-	tr	m to tr	M
chalcopyrite	tr to m	-	tr	m	M
isocubanite	tr	-	-	tr	tr
galena	tr	-	-	m	tr
arsenopyrite	tr	-	-	-	-
barite	- to tr	A	A	tr	m
bitumen	-	M	-	-	-
amorphous silica	-	m to M	M	M	M
clay	m	M	M	M	m
chlorite	- to tr	-	-	-	-
sulphosalts	-	-	-	-	tr
covellite	-	-	-	-	tr
iron oxides	-	-	-	-	m
Pore space	25-65	20	50	20	40

A=abundant (>40 vol. %), M=major (5-40 %) m=minor (1-5%), tr=trace (<1%),

Area of Active Venting: active anhydrite chimneys

Nine active chimneys were sampled from the AAV from Dead Dog Mound, Heineken Hollow, East Hill, Central Site, Chowder Hill and Inspired Mound. Actively venting chimneys from the AAV typically have a 2-mm-wide clay-rich inner lining with finely disseminated sulfides, and a thick (>10 cm) outer wall composed primarily of anhydrite (Figs. 5A, B, 6A, B, C). In order of abundance, the sulfides present in the clay-rich inner wall are chalcopyrite, pyrrhotite, sphalerite, isocubanite, pyrite, marcasite, galena and arsenopyrite (<10% modal abundance combined). Pyrrhotite, chalcopyrite, and trace isocubanite are characteristic of the high-temperature vents. Gypsum (and bassanite) are locally abundant in some chimney samples, but these are secondary products formed by the hydration of anhydrite following sample recovery.

Clay minerals show micrometric concentric zoning within the inner wall (Fig. 6B). Individual bulbous lobes average 45 μm in cross-section (Fig. 6D). The layers of clay radiate out toward the fluid channelway, with colloform bands of alternating clay-rich and thinner sulfide-rich bands (Fig. 6B). Clay casts of dissolved lath-shaped anhydrite occur at the contact between the inner and outer walls of chimney samples, within fossil channelways in the outer anhydrite zone of chimneys and within the mounds (Figs. 6C, E). The clay minerals, identified by X-ray diffraction (XRD), electron-microprobe analyses and transmission electron microscopy (TEM) studies, include a variety of smectite-group minerals, dominated by saponite, with less abundant cobalt-bearing smectite, Fe-rich saponite and Fe-rich smectite (Percival & Ames 1993) (Fig. 6B). Chlorite and Fe-rich smectite form the clay-rich lining of the highest-temperature vent on Chowder Hill (Percival & Ames 1993).

Chalcopyrite is the dominant sulfide phase in the core of the active chimneys and typically occurs along growth zones between lobes of Mg-bearing smectite (Fig. 6B). These growth zones suggest fluctuating chemical or physical conditions (or both), and are indicative of a series of fluid pulses. Chalcopyrite and minor isocubanite are commonly intimately intergrown with sphalerite, and these phases are interstitial to pyrrhotite plates. Within the active chimneys, the chalcopyrite–isocubanite is very fine-grained, typically 2–5 μm, but at East Hill the chimney contains coarser chalcopyrite, with individual grains up to 0.2 mm. Sphalerite and chalcopyrite occur together in the highest-temperature chimneys, and are mutually intergrown. Sphalerite grains in the chimney samples are opaque owing to a high iron content (see microprobe data below). Pyrrhotite occurs as blades or laths, typically as a network of randomly oriented, interpenetrating crystals in open spaces or disseminated within Mg-bearing smectite. The pyrrhotite blades are 3 μm to 2 mm in length, but typically attain 100 μm,

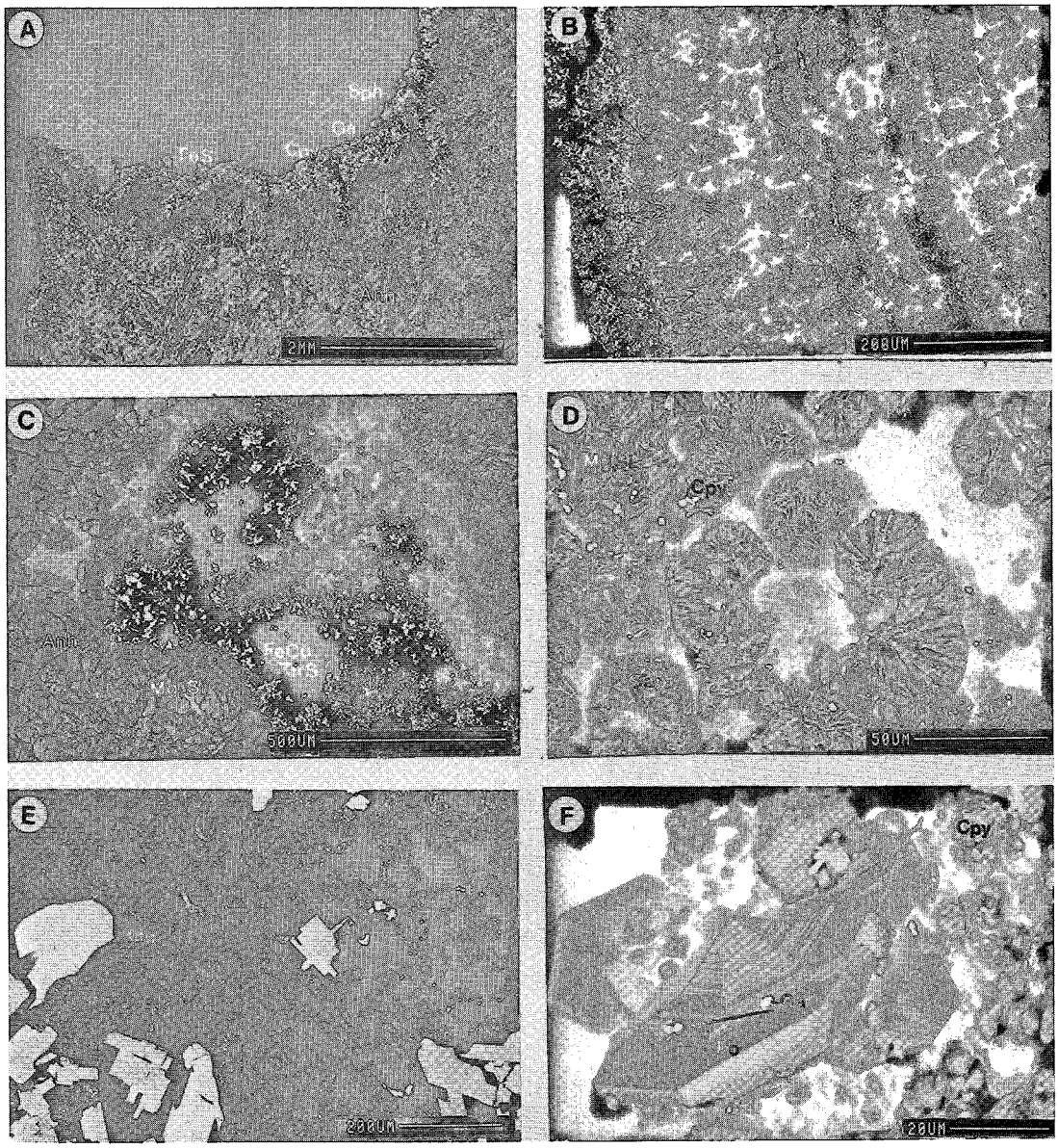

FIG. 6. Scanning electron micrographs of active chimneys at Middle Valley. A. Back-scattered electron (BSE) image of a section across an active chimney. The central orifice is on the upper left. At the contact between the anhydrite-rich (Anh) outer zone and the sulfide-rich lining (bright grains) is a narrow grey zone with saponite (Mg, Si) casts of dissolved anhydrite laths. Sample 2251–1–1. B. Close-up BSE image of the inner lining of the active chimneys, with the fluid pathway to the left. Note the alternating colloform growth of the radiating saponite and fine grain-size of the sulfides. Sample 2251–2–3. C. Note the replacement of anhydrite by Mg-rich smectite (Mg, Si) within fluid pathways in the anhydrite-rich outer zone. Sample 2251–2–3. D. Secondary electron image of a plan view of the inner lining of the Dead Dog active chimney. Forty-μm Mg-rich smectite (saponite) lobes with finely disseminated chalcopyrite. Sample 2251–1–1. E. BSE close-up image of a saponite–sulfide band within the anhydrite-rich outer carapace. The saponite forms casts of anhydrite. Sample 2251–2–3. F. Secondary electron image of euhedral pyrrhotite (Po) crystals with inclusions of galena (ga). Sample 2251–1–1.

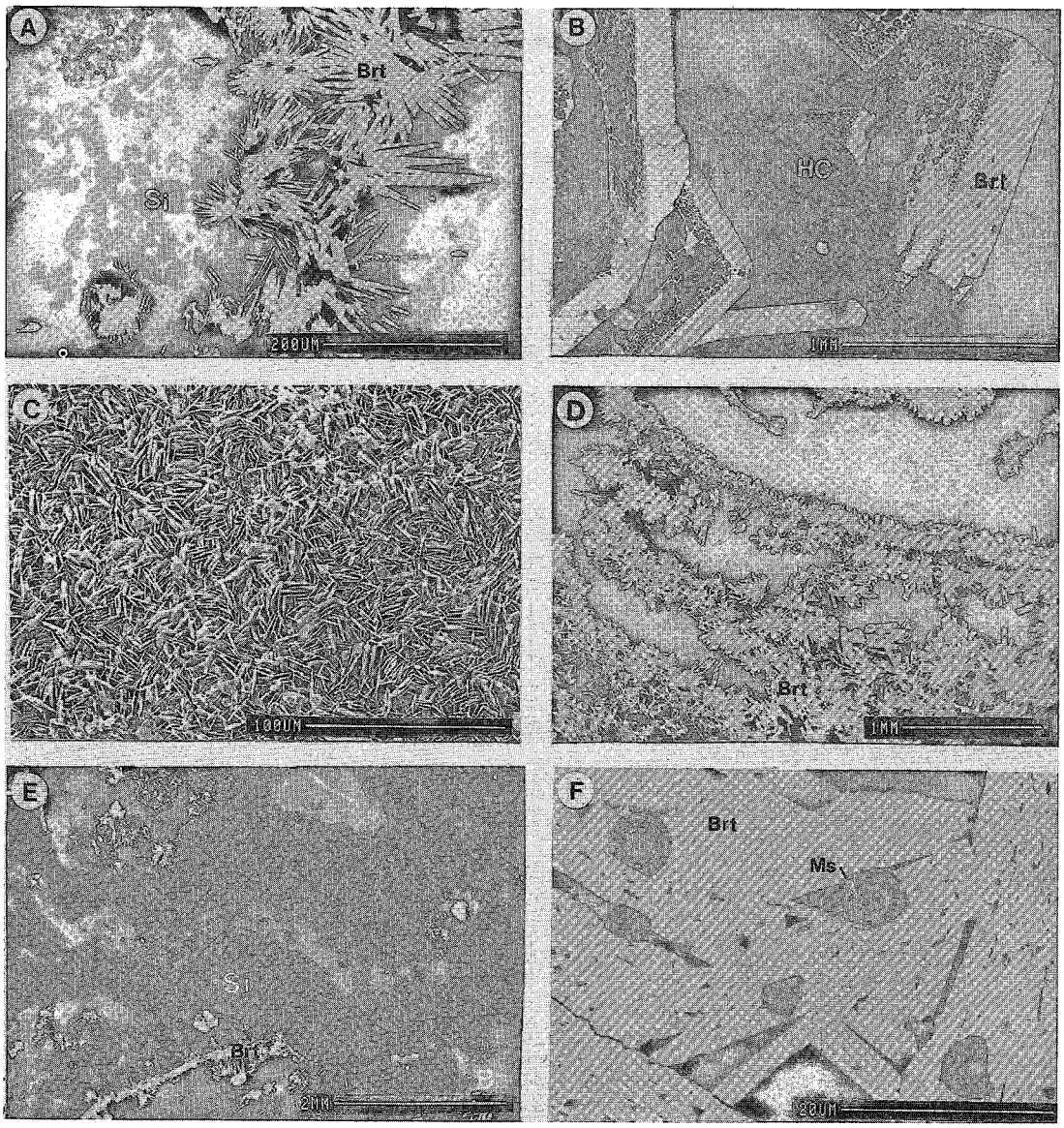

FIG. 7. Scanning electron micrographs of inactive chimneys and barite crusts at Middle Valley. A. BSE image of radiating barite crystals (Brt) coated with amorphous silica (Si). Sample 2252–2–1a. B. Hydrocarbons (black, HC) form between barite (Brt), as inclusions in barite crystals and as secondary inclusions of liquid hydrocarbon. Sample 2255–3–2a. C. Secondary electron image of a fragment from the barite-rich crust at Heineken Hollow. Note the dense interlocking texture. Sample 2251–2–1. D. BSE image of arcuate narrow filaments or tubes forming the nucleus for rosettes of barite (Brt). Sample 2251–2–1. E. BSE image of veinlets of amorphous silica (Si) that cross-cut the barite-rich altered sediment. In the silica-rich veinlets are foraminifera casts and rectangular rods of silica. Sample 2251–2–1. F. BSE image of colloform marcasite (Ms) contemporaneous with barite forming within and between tabular crystals of barite. Sample 2251–2–1a3.

with aspect ratios (length:width) of 5:1. The higher temperature (276°C) vent at Chowder Hill contains the coarsest pyrrhotite. Trace amounts of galena occur in the active chimneys as 2–5 μm inclusions within hexagonal pyrrhotite (Fig. 6F). Isolated 20–100 μm crystals of galena also occur along fractures in anhydrite and are slightly more abundant (1% modal abundance) in the East Hill chimney. Minor chalcopyrite may occur locally along fractures in galena. Trace amounts of arsenopyrite occur in the Mg-bearing smectite–sulfide inner lining of the active chimney at Dead Dog Mound. Grains of arsenopyrite are 5 μm in diameter and occur adjacent to pyrrhotite plates and as a fine, ragged open-space growth on pyrrhotite plates. Rare framboidal or cubic grains of pyrite also are present.

The porosity in the sulfate-rich outer zone is high, from 25 to 65%. Anhydrite is present as 1 mm to 3 mm euhedral tablets and in rare rosettes (Figs. 6A, C). Trace amounts of barite are disseminated within the outer zone as 25 μm radiating rosettes or 70 μm blocky grains in cross-section. Channelways for the fluid transect the anhydrite zone and are lined with clays, sphalerite and chalcopyrite.

Area of Active Venting: inactive chimneys

Although the AAV hosts numerous vents, there are more inactive than active chimneys. Inactive chimneys are most abundant on the east side of the southern part of the field and between Central Site and East Hill (Fig. 3A). Two inactive barite-rich chimneys from east of Dead Dog Mound and one inactive chimney south of East Hill were studied. A complete barite chimney (2255–3–2,2A) and altered mud from its base were recovered (Figs. 3A, 5C). The inactive chimneys are composed predominantly of barite and subequal amounts of amorphous silica, and minor clay and marcasite. They have less pore space (about 20%) than the active chimneys, and are commonly impregnated with hydrocarbons identified as hydrothermal bitumen (Simoneit *et al.* 1992). The inactive chimneys are concentrically zoned, with thin barite bands alternating with mixtures of bitumen and clay minerals (Fig. 5D).

Barite is the dominant phase and occurs as rosettes 0.7 mm in length and as isolated grains between clay aggregates. Clay minerals occur in open spaces and between barite crystals in the inactive chimneys as subrounded, anhedral 1.2 mm blebs and spherical radiating crystals in 4-mm aggregates. Amorphous silica forms colloform layers and globular coatings on the earlier-formed minerals and infills the pore space between the clays and barite (Fig. 7A). The silica coating is typically 0.02 mm thick. Veinlets of silica also cross-cut barite. Globules of hydrothermal bitumen, as large as 1 mm, occur in fractures between barite, and trapped inclusions of liquid hydrocarbon are found in the barite (Fig. 7B). Square cavities in barite, filled with bitumen, are progressively smaller, from 100 μm to 10 μm, from the core to the rim of a crystal. Much of the trapped bitumen has squeezed out along grain boundaries as a result of decompression during transport of the samples to the sea surface.

Area of Active Venting: barite crust

Deposits of barite adjacent to the low-temperature active vent in Heineken Hollow form a yellowish crust on top of the hemipelagic sediment (Figs. 5E, F). The crust consists principally of a porous network of lacey barite filaments with 50% open space, 10% amorphous silica, trace marcasite, and 5–10% altered sediment (Fig. 7C). Euhedral barite partly infills the open spaces. Filamentous rods, 3 mm in length, are the nucleus for radiating rosettes of barite (Fig. 7D). The core of the barite filaments is commonly brown in plane-polarized light, and contains hemipelagic silt and clays. Some barite has grown on biological material. Rare spheres of barite occur in the open spaces between blocky grains of barite. Amorphous silica occurs as broken rods, semicircular, anhedral and bulbous accumulations and veins. The silica locally contains casts of foraminifera (Fig. 7E) and apparent tubular structures that may be the fossilized remains of vent-related worm tubes. Trace amounts of colloform marcasite occur in the core of barite rosettes and form triangular growths between crystals of barite (Fig. 7F).

Area of Active Venting: active mounds

The hydrothermal mounds that host active chimneys consist of toppled chimney material and hydrothermally altered sediment in a matrix of primary hydrothermal precipitates. Much of the sedimentary and chimney material is replaced by secondary clays and infilled with interstitial silica and sulfide. These mounds are the sites of considerable hydrothermal replacement and overprinting (Fig. 8). The primary compositions of the earlier hydrothermal products are therefore difficult to ascertain. Three hydrothermal mounds were studied: Dead Dog Mound, Chowder Hill and Central Site.

Hand specimens of altered chimney debris consist of a very porous, interlocking network of yellowish green needles of clay minerals that are pseudomorphic after anhydrite. The secondary clays also form casts as 0.1 to 0.2 mm bulbous overgrowths on the original 2- to 4-mm-long laths of anhydrite (Fig. 8A). The original clay–sulfide assemblage, probably from the inner walls of active chimneys, has retained its original colloform texture, but is more dense owing to later deposition of sulfides, with up to 30% chalcopyrite and sphalerite as <10 μm grains. Rare laths of altered pyrrhotite contain 1-μm inclusions of galena.

Silica, Mg-bearing smectite, pyrite, marcasite, gale-

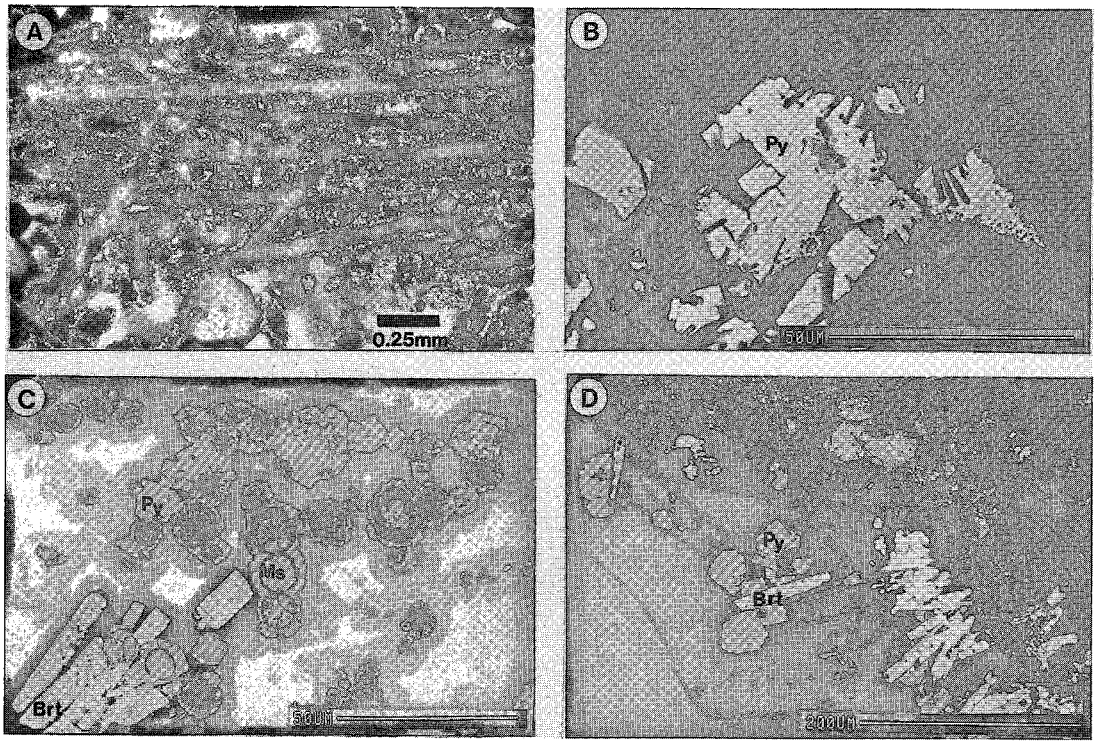

FIG. 8. Textural features within hydrothermal mounds at Middle Valley. A. Pseudomorphic replacement of anhydrite laths by Mg-rich smectite. Mg-rich smectite also occurs as fine bulbous rims on the laths as casts of anhydrite. Transmitted light, sample 2252–4–1c. B. BSE image of secondary silica (Si) and pyrite (Py) overgrowths on fine lath-shaped voids. Note the dissolution features in the pyrite. Sample 2252–4–1b. C. Low-temperature phases with barite, colloform marcasite and pyrite rimmed by amorphous silica. BSE image, sample 2252–4–1b. D. Partial to total dissolution of barite (Brt). Casts of silica retain barite morphology. BSE image, sample 2252–4–1b.

na and barite are the principal precipitates filling open spaces within the mound. Secondary amorphous silica comprises up to 25% of the interstitial mound material, commonly cementing the mound rubble. Spheres of amorphous silica form a coating over the lower-temperature phases, such as colloform marcasite, barite and hydrothermal Mg-bearing smectite. Up to 15% pyrite is present as anhedral and rare euhedral crystals and as partially corroded grains (Fig. 8B). Colloform marcasite is present locally (Fig. 8C). Minor colloform bands of interlayered pyrite, barite and marcasite are observed; in most cases, marcasite is pseudomorphic after pyrite. Relict barite may occur in the late silica, but more commonly the barite is completely dissolved, leaving only casts or lath-shaped voids lined by silica (Fig. 8D). Radiating laths of barite are commonly rimmed by pyrite and subsequently by 0.1-mm amorphous silica.

A push-core sample was collected at the top of the mound immediately adjacent to the Central Site active vent, where low-temperature (100°C) fluid was discharging (Turner *et al.* 1993). The core contains mineral assemblages typical of relatively low-temperature venting; saponite, coarse-grained galena, chalcopyrite, sphalerite and pyrite. The ratio of base metal sulfides to iron sulfides is high (Turner *et al.* 1993). Saponite, lizardite and a serpentine–smectite mixed-layer mineral form the matrix (Percival & Ames 1993). The sphalerite crystals are honey-colored and zoned, with a slightly darker core. Chalcopyrite occurs as isolated grains or intergrown with sphalerite. Galena is coarser and more abundant in the Central Site mound than in any of the other hydrothermal deposits at Middle Valley. Anhedral and corroded (100 µm) grains of galena are disseminated within the saponite and serpentine–smectite mixture.

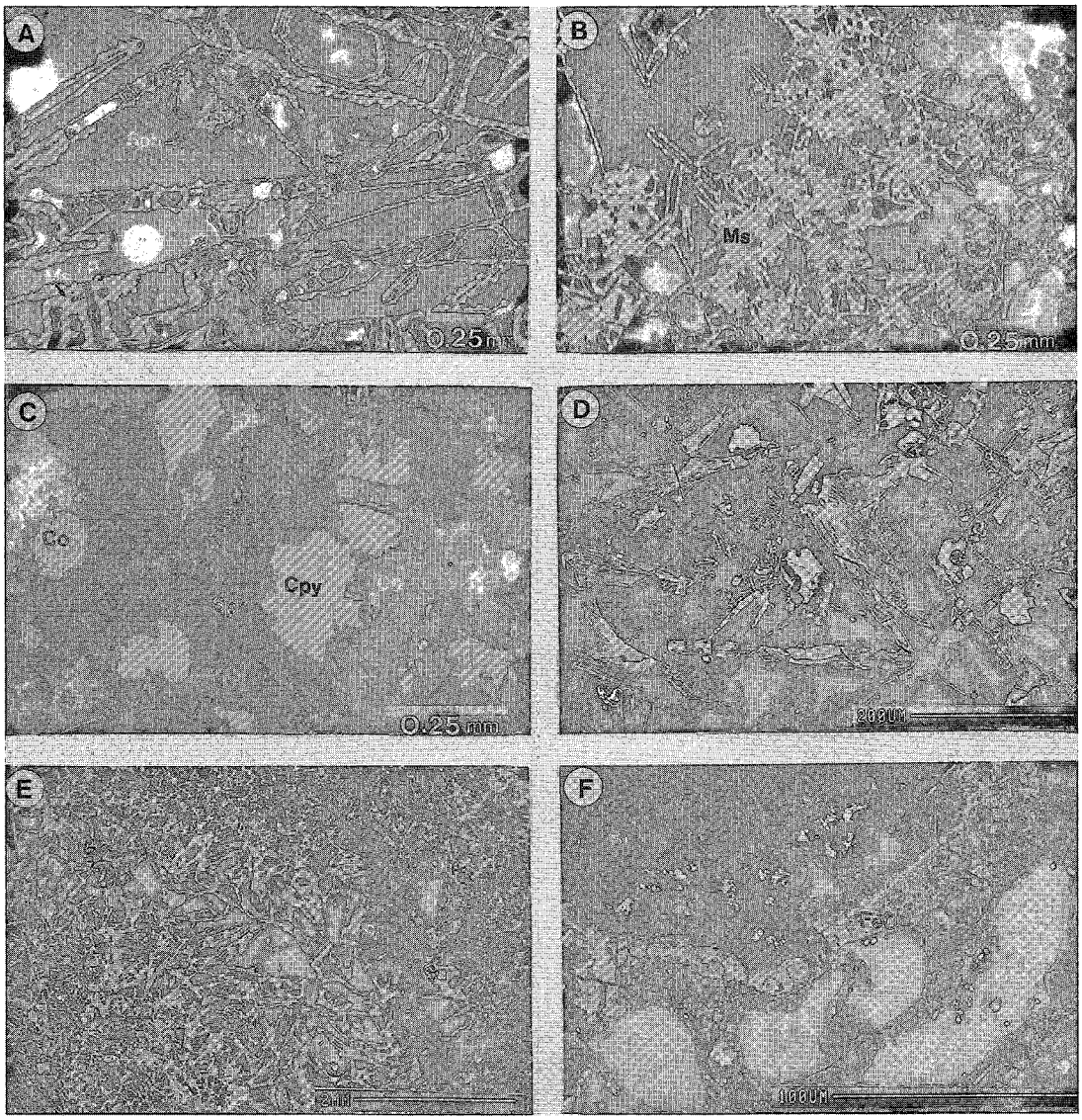

FIG. 9. Textural features of sulfide outcrop at southern Bent Hill. A. Lepidocrocite pseudomorphically replaced pyrrhotite laths, and secondary marcasite (Ms) and pyrite (Py) rim the lepidocrocite. Sphalerite (sph) and chalcopyrite (cpy) are interstitial to the laths. Reflected-light photomicrograph of sample 2253–1–3. B. Marcasite (Ms) forms casts of pyrrhotite–lepidocrocite laths, with mineral growth along cleavage planes. Reflected-light photomicrograph of sample 2253–1–3o. C. The massive sulfide is denser owing to coarse sphalerite (Sph) and chalcopyrite (Cpy) infilling pore space between lepidocrocite laths. Chalcopyrite is partially altered to covellite (Co). Reflected-light photomicrograph of sample 2252–1–3o. D. BSE image showing amorphous silica (Si) in the interstices between lepidocrocite laths, sphalerite, and chalcopyrite grains decreases the pore space. Sample 2253–1–1. E. The massive sulfide, denser owing to coarsening sphalerite and chalcopyrite and cementation by amorphous silica and marcasite, is cross-cut by veins rich in silica (Si) and galena (Ga). BSE image of sample 2251–1–3. F. Pb–As–Sb sulfosalts (Ss) associated with silica occur at the outer oxidized rim of the massive sulfide outcrop. The outer rim is composed of barite, marcasite, Fe-oxides (FeO) and amorphous silica. BSE image 2253–1–3o.

Bent Hill: sulfide outcrop

The sulfide samples from the south flank of Bent Hill differ significantly from the active chimneys in the AAV. Much of the sulfide outcrop consists of massive pyrrhotite, lepidocrocite, pyrite, marcasite and sphalerite, with minor chalcopyrite, covellite, galena, silica and barite. Unlike the active chimneys in the AAV, where pyrrhotite is the dominant Fe-sulfide, samples from the sulfide outcrops at Bent Hill are composed of pyrrhotite–pyrite. The massive sulfides are dense (<15% pore space), with Cu and Zn sulfides and late amorphous silica cementing early pyrrhotite. In addition, the sulfides show evidence of extensive recrystallization and coarsening, secondary replacement, and seafloor weathering, consistent with the apparently older age of the deposits. These deposits have apparently been affected by multiple generations of hydrothermal fluid.

Original massive pyrrhotite (up to 35 vol.%) from the sulfide outcrop comprises a network of coarse-grained (50 μm), interpenetrating blades or laths, commonly with a rim of pyrite. The oxidized remnants of pyrrhotite-rich sulfides (Fig. 9A) consist of fibrous lepidocrocite. At the outer edge of the outcrop, the pyrrhotite has been completely destroyed, leaving lath-shaped voids rimmed by amorphous silica or marcasite (Fig. 9B). Pyrite is preserved in the interstices of the remnant laths of pyrrhotite.

Coarse sphalerite (0.25 mm) occurs between the pyrrhotite laths and is generally opaque. Chalcopyrite occurs as isolated grains and as inclusions with delicate serrate edges within sphalerite (Fig. 9C). "Chalcopyrite disease" is common. Chalcopyrite in the massive sulfide is coarser (0.1–0.3 mm) than that precipitated in the inner lining of all of the active chimneys and is more abundant (5% modal abundance). Covellite occurs locally as a product of secondary replacement of chalcopyrite and forms randomly oriented crystals adjacent to coarse sphalerite and chalcopyrite and within sphalerite (Fig. 9C). Late amorphous silica (25–35% modal abundance) forms 10 μm colloform coatings on the sulfide minerals and cements the massive sulfides (Fig. 9D). Silica also occurs in late cross-cutting veinlets. Galena is spatially associated with late-stage silica within the massive sulfides and is commonly corroded (Fig. 9E).

Samples of the massive sulfide mound and associated sulfide talus are mineralogically zoned, with an outer rim of goethite, barite, galena, marcasite, amorphous silica and Pb–As–Sb sulfosalts. This assemblage is believed to have been associated with a stage of low-temperature venting that reworked the massive sulfide mound. The barite typically forms coarse, radiating overgrowths on the massive sulfides, together with abundant colloform marcasite and coarse (50–100 μm), euhedral galena. Amorphous silica commonly forms coatings 0.5–1 mm thick on the barite and locally contains fine, 1–5 μm inclusions of sulfosalts (Fig. 9F).

Most of the mineral textures in the sulfide deposits at Bent Hill are secondary, and much of the original pyrrhotite has been pseudomorphically replaced by iron oxides and sulfides. Extensive reworking is illustrated by late veining, infilling of pore space by coarse sphalerite, chalcopyrite and abundant silica, partial and total replacement of pyrrhotite, corroded galena in the massive sulfide and euhedral galena in silica veins, and the distribution of Pb–Sb–As sulfosalts on the outer rim of the massive sulfide samples. Oxidation of chalcopyrite to covellite and local replacement of pyrrhotite by pyrite and marcasite also suggest that more than one generation of fluid has percolated through the sulfide deposit.

Bent Hill: active chimney

A single chimney venting fluid at 264°C occurs on the southernmost sulfide outcrop (Figs. 4A, B). A sample from the active chimney resembles those from the AAV, with a thick outer wall of anhydrite and a thin inner wall of clay, and disseminated grains 2–20 μm across of pyrrhotite, chalcopyrite, sphalerite and trace barite (sample 2253–1–5, Fig. 4B). As in the AAV, the active chimney appears to be a product of relatively sulfur-depleted solutions. The presence of an active vent of this type on top of the sulfide outcrop suggests that the massive sulfide deposits south of Bent Hill are currently being flushed by hydrothermal fluids similar to those venting in the AAV.

Mineral Compositions

Electron-microprobe analyses of silicate and sulfide minerals were obtained for the various hydrothermal deposits in Middle Valley. The results for sphalerite are shown on Figure 10; results of analyses of pyrrhotite, isocubanite, chalcopyrite, galena and barite are listed in Tables 3 to 7, respectively. Clay-mineral

TABLE 3. ELECTRON MICROPROBE DATA ON PYRRHOTITE FROM MIDDLE VALLEY

	Fe	Ni	Co	Mn	Cu	S	Total
Active chimney Dead Dog Mound 2251-1-1a n=10	61.85	0.01	0	0.02	0.08	37.18	99.14
Sulphide outcrop site 856 2253-2-1d n=3	60.80	0.02	0	0.03	0.76	37.95	99.56

concentrations in wt. %

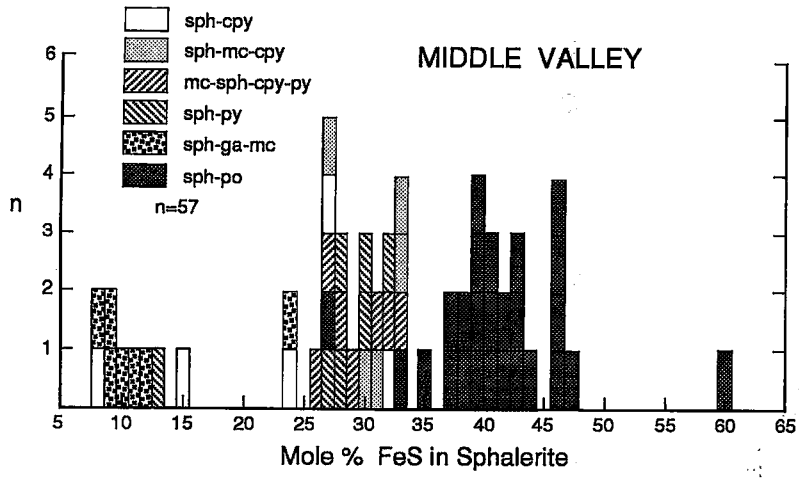

FIG. 10. Histogram of mole % FeS in sphalerite and Fe–Zn sulfides from Middle Valley. The associated sulfide phases are noted. Symbols: sph sphalerite, cpy chalcopyrite, mc marcasite, py pyrite, po pyrrhotite, ga galena.

analyses from the active chimneys and from one mound are discussed in Percival & Ames (1993), and the clay compositions obtained from the shallow sediments close to active vents are listed in Turner *et al.* (1993).

Three distinct populations of sphalerite are apparent, based on iron contents (Fig. 10). Iron-rich sphalerite (35–47 mole % FeS) is associated with pyrrhotite (± isocubanite) in the inner lining of the active chimneys from the AAV (*e.g.*, Chowder Hill, Dead Dog Mound, Heineken Hollow). Low-iron sphalerite (<15 mole % FeS) is associated with marcasite and galena in the active mound carapace at the Central Site and at East Hill. This assemblage is interpreted to have formed at a relatively low temperature and may be related to the current phase of venting or an earlier, lower-temperature phase. Pyrite–pyrrhotite assemblages in sulfide talus south of Chowder Hill and in the Inspired Mounds chimneys contain sphalerite with moderate levels of iron, *i.e.*, 24–33 mole % FeS. This assemblage resembles material from the sulfide outcrops at Bent Hill, which contains coexisting pyrite, marcasite, and lepidocrocite (formerly pyrrhotite). Sphalerite from the sulfide outcrops at Bent Hill also contains 24–33 mole % FeS. The large variation in sphalerite composition in different parts of Middle Valley reflects the large temporal and spatial variability in fluid compositions. In most seafloor deposits, iron-rich sphalerite typically forms at high temperatures and low $a(O_2)$ and $a(S_2)$; sphalerite with lower iron contents forms at lower temperatures and from relatively more oxidized solutions (Hannington & Scott 1989).

Pyrrhotite compositions were determined in samples from Dead Dog Mound (AAV) and Bent Hill (Table 3). Pyrrhotite from the active vent on Dead

TABLE 4. ELECTRON MICROPROBE DATA ON ISOCUBANITE FROM MIDDLE VALLEY

	Cu	Fe	Pb	Ni	Co	Mn	Zn	As	S	Total
Active chimney										
Dead Dog Mound										
2251-1-1a	19.08	43.58	0	0	0	0.10	1.22	0.05	34.60	98.63
Sulphide outcrop										
South of Bent Hill										
2253-1-3o	19.66	40.48	0	0.09	0.07	0.05	1.72	0.27	35.00	97.34

concentrations in wt. %

TABLE 5. ELECTRON MICROPROBE DATA ON CHALCOPYRITE FROM MIDDLE VALLEY

	Cu	Fe	Pb	Ni	Co	Mn	Zn	As	S	Total
Diffuse venting										
Clam Area-Mound										
2252-4-1c	30.93	32.37	0	0.02	0.02	0	0.47	0.10	33.54	97.45
Active chimney										
Inspired Mound										
2255-4-2a	30.93	28.61	3.21	0	0.03	0.10	2.03	0.90	32.50	98.31
Mound										
Central Site										
2255-5-1PT1	33.98	29.44	0	0.01	0.07	0	0.31	0	34.37	98.18
	33.90	30.04	0	0.01	0	0.02	0.27	0	34.23	98.47

concentrations in wt. %

Dog Mound contains 48.3–50.0 at.% Fe, and that from the sulfide outcrop at Bent Hill contains 47.3–47.9 at.% Fe. The different compositions of pyrrhotite from these sites are consistent with bulk mineralogy (*i.e.*, pyrrhotite-dominant assemblages at AAV *versus* pyrrhotite–pyrite assemblages at Bent Hill) and the iron content of associated sphalerite.

Isocubanite in the high-temperature chimneys from the AAV and in the sulfide outcrop at Bent Hill is close to stoichiometric $CuFe_2S_3$ (Table 4). It is commonly in intimate association with pyrrhotite and chalcopyrite, and generally occurs together with high-iron sphalerite (*e.g.*, 46 mole % FeS in sphalerite from a pyrrhotite – sphalerite – isocubanite chimney on Dead Dog Mound). Textural relations among these phases suggest that Cu–Fe sulfide was precipitated as an intermediate solid-solution (*Iss*), which has subsequently exsolved chalcopyrite and isocubanite. The high Zn(S) content in isocubanite may have been present in solid solution in the original high-temperature *Iss* (Scott 1983).

Chalcopyrite from the AAV is stoichiometric $CuFeS_2$, with traces of Zn, Co and As (Table 5). The high levels of Zn and Pb in sample 2255–4–2a likely reflect the presence of microscopic inclusions of sphalerite and galena, which are common in chalcopyrite from this site.

Galena from one sample in the AAV contains no traces of As, Sb, Ag, Bi, or Cu (Table 6). However, qualitative analysis of the sulfosalt phase, present in trace amounts on the outer crusts of sulfide samples from the Bent Hill, was possible with the use of a scanning electron microscope with energy-dispersion spectrometry. It was found to contain Ag, As and Sb.

Barite from a 254°C anhydrite chimney near East Hill contains only 0.64 wt.% SrO (Table 7). In inactive chimneys and barite-rich crusts from the AAV, barite contains 1.43–1.57 wt.% SrO. Barite from sulfide talus in the Bent Hill area is similar in composition to barite from the inactive chimneys and barite-rich crusts in the AAV. Goodfellow & Blaise (1988) noted a wide range of Sr contents (up to 11.6 wt.% SrO) in barite from shallow, 2-m-long piston cores in the Bent Hill area. The variability of Sr/Ba ratios in barite from Middle Valley may reflect variable contributions of sediment-derived Sr during hydrothermal venting (*e.g.*, Campbell *et al.* 1992).

TABLE 6. ELECTRON MICROPROBE DATA ON GALENA FROM MIDDLE VALLEY

Central Site Mound, 2255-5-1PT1, n=12

	MEAN	S.D.		MEAN	S.D.
Pb	85.69	0.56	Bi	0.02	0.03
Ag	0.04	0.02	Cu	0.08	0.19
As	0.02	0.02	Fe	0.14	0.10
Sb	0.05	0.03	S	13.40	0.11
Total	99.44				

concentrations in wt. %

TABLE 7. ELECTRON MICROPROBE DATA ON BARITE FROM MIDDLE VALLEY

	BaO	SrO	CaO	MnO	MgO	FeO	SO3	Total
Active Chimney 2255-6-1B n=3	66.15	0.64	0.17	0.12	0.05	0.05	32.57	99.75
Barite crust 2251-2-1A n=9	66.66	1.57	0.56	0.10	0.03	0.02	31.64	100.58
Barite chimney 2254-23-1 n=15	63.89	1.43	0.07	0.12	0.04	0.07	33.75	99.36
Sulphide talus 2253-1-1 n=10	63.52	1.81	0.05	0.09	0.06	0.11	33.76	99.40

concentrations in wt. %

GEOCHEMISTRY

Whole-rock and trace-element chemical data for Middle Valley chimneys, barite crusts, massive sulfides and altered sediment are listed in Tables 8 and 9. Active chimneys and barite-rich inactive chimneys and crusts have low metal contents, owing to the abundance of non-sulfide phases (anhydrite, barite, silica, clays). Active chimneys in the AAV and Bent Hill are dominated by anhydrite, amorphous silica, and clays (98 wt%). Chemical analyses of the inactive chimneys

TABLE 8. GEOCHEMISTRY OF ACTIVE AND INACTIVE CHIMNEYS, BARITE CRUST AND ALTERED MUD IN THE AAV, MIDDLE VALLEY.

	ACTIVE CHIMNEYS						INACTIVE CHIMNEY	BARITE CRUST	ALT MUD
Site	DDM	DDM	IM	HH	EH	CH	east of DDM	HH	east of DDM
T.°C	265	268	253	184	254	276	-	-	-
Sample (225)	1-1-1A	1-1-1	5-4-2	1-2-3	1-3-2	2468-1	5-3-2	1-2-1b	5-3-2a
(wt.%)									
SiO_2	6.54	6.72	2.56	7.35	5.21	1.17	8.02	75.0	63.9
TiO_2	<0.02	<0.02	<0.02	<0.02	<0.02	<0.02	<0.02	0.14	0.43
Al_2O_3	0.27	0.25	0.05	0.34	0.27	0.02	0.70	2.71	8.35
Fe_2O_{3T}	0.52	0.59	0.52	0.72	0.55	3.53	0.24	1.29	4.25
MnO	0.01	0.01	0.01	0.02	0.01	0.01	0.02	0.02	0.13
MgO	4.12	3.61	1.44	4.36	2.54	0.65	0.11	0.64	2.50
CaO	37.0	38.1	40.0	37.5	37.7	37.5	0.34	2.37	1.21
Na_2O	0.43	0.45	0.54	0.52	0.57	0.45	0.45	1.14	3.41
K_2O	0.11	0.12	0.14	0.12	0.12	0.06	0.17	0.53	0.53
C	-	-	-	-	-	-	4.30	0.30	0.60
S	21.2	21.6	23.2	20.9	22.0	23.6	12.14	3.61	1.01
Au (ppb)	9	4	18	80	7	51	335	80	859
Ba (ppm)	120	210	550	100	170	370	36%	2%	2.7%
Ag	<2	<2	4	<2	<2	<2	12	5	<2
Cu	1300	1100	1600	1500	1100	210	17	76	150
Zn	230	440	1600	400	570	1500	2	51	87
Pb	28	68	700	50	130	7522	22	17	34
As	4.2	1.4	7	0.7	1.8	29	8	33.4	58.7
Sb	0.3	0.3	3.3	0.2	0.5	2.2	6.5	3	3.4
Se	2	2.9	15.6	2.8	4.7	11	29.8	8.4	6.2
B	9.3	8.3	9.1	8.7	5.3	-	5.3	30.2	68.0
Be	0.6	0.6	0.7	0.7	0.6	<0.5	0.70	1.2	1.7
Co	<5	<5	<5	<5	<5	<5	7	7	14
Cr	<10	<10	<10	<10	<10	<10	<10	20	59
Ni	<10	<10	<10	<10	<10	<10	<10	<10	<10
Sr	1700	1500	1400	1700	1500	1700	3300	2300	630
V	<5	<5	<5	<5	<5	<5	9	44	93
Y	1	1	2	2	<5	<5	<5	<5	10
Zr	<20	<20	<20	<20	<20	<20	<20	23	74

DDM=Dead Dog Mound, IM=Inspired Mounds, HH=Heineken Hollow, EH=East Hill, CH=Chowder Hill, ALT=Altered.
Analyses done by Geological Survey of Canada laboratories except Au; by Neutron Activation Analyses, RMC, Kingston.

TABLE 9. GEOCHEMISTRY OF ACTIVE CHIMNEY, SULFIDE DEPOSIT AND ALTERED MUD IN THE BENT HILL AREA, MIDDLE VALLEY

	ACTIVE CHIMNEY		MASSIVE SULFIDE			SEDIMENT	
Site	South Bent Hill	Talus	Outcrop	Outer Crust	Outcrop		Top of Bent Hill
Temp.°C	264	-	-	-	-	-	-
Sample (2253-)	1-5	1-1	1-4	1-4a	1-3	3-2	4-1
(Wt.%)							
SiO_2	0.33	-	68.5	-	1.73	-	58.5
TiO_2	<0.02	-	<0.02	-	<0.02	-	0.82
Al_2O_3	0.02	-	1.28	-	0.08	-	15.9
Fe_2O_3T	3.53	18.2*	12.9	18.6*	41.5	0.17*	9.27
MnO	0.01	-	0.11	-	0.03	-	0.10
MgO	0.65		0.16	-	0.08	-	4.21
CaO	37.5		0.16	-	0.09	-	37.7
Na_2O	0.45	0.47*	0.65	0.55*	0.69	0.33*	3.01*
K_2O	0.06	-	0.14	-	0.17	-	2.97
C	-	-	0.20	-	0.20	-	0.20
S	23.8	-	10.83	-	39.40	-	0.09
Au(ppb)	51	350	34	300	3890	335	-
Ba(ppm)	370	0.31%	3%	0.41%	1%	47.6%	0.78%
Ag	<2	140	13	36	32	20	<2
Cu	210	-	51	-	18000	-	64
Zn	1500	10500	600	1860	36000	<50	180
Pb	75	-	580	-	150	-	23
As	29	83	119	850	35.2	9.8	5.8
Sb	2.2	96	35.2	206	60.2	12	0.8
Se	11	97	2.1	2	10.1	-	<0.2
B	-	-	-	-	-	-	89.8
Be	<0.5	-	0.1	-	0.1	-	2.1
Co	<5	<5	<5	<5	9	<5	19
Cr	<10	-	<10	-	<10	-	98
Ni	<10	-	<10	-	13	-	72
Sr	1700	-	270	-	6	-	220
V	<5	-	<5	-	<5	-	120
Y	<5	-	<5	-	<5	-	22
Zr	<20	-	<20	-	<20	-	130

Analyses done by Geological Survey of Canada laboratories except Au; by Neutron Activation Analyses, RMC, Kingston. Partial analyses also by NAA
* = elemental form (Fe, Na).

also reflect the major mineral phases, with up to 38 wt% Ba present as barite, 8.0 wt% SiO_2 as amorphous silica, and up to 4.3 wt% C as secondary hydrocarbons. The high Mg and Al in a number of samples reflect the local abundance of clay minerals. Despite low metal contents, the presently active chimneys from the AAV and massive sulfides from Bent Hill are clearly distinct on the basis of bulk Cu:Zn ratios (Fig. 1). Sulfides from active chimneys in the AAV have high average Cu:Zn ratios of about 5:1, whereas sulfides from the older Bent Hill deposits have a Cu:Zn ratio of less than 1. The inactive chimneys and barite-rich crusts in the AAV also have low Cu:Zn ratios. Pb/(Cu+Zn) ratios in the Middle Valley chimneys are generally higher than in massive sulfides from bare-ridge deposits (Fig. 11).

Significant levels of Ag, As, and Sb are present in a few of the low-temperature sulfide assemblages from Bent Hill, with maximum measured concentrations of 140 ppm Ag, 120 ppm As, and 96 ppm Sb. One sample of the low-temperature, SiO_2-rich crust containing Pb–As–Sb sulfosalts contains 850 ppm As and 200 ppm Sb. Although bulk As concentrations are low in the active chimneys, trace arsenopyrite was identified in one sample.

The bulk gold contents of active chimneys in the AAV are uniformly low, with a maximum of 80 ppb Au. Gold concentrations in these samples are diluted by the abundant non-sulfide phases, and gold concentrations within individual sulfides could be as much as two orders of magnitude higher (*i.e.*, ppm concentrations). Bulk gold contents in the barite-rich chimney material and barite crusts are 335 and 80 ppb Au, respectively. Four sulfide-rich samples from the Bent Hill area average close to 1 ppm Au, which indicates locally significant enrichment of gold. One sample of altered sediment at the base of the inactive chimney from the AAV also is notably enriched in gold (859 ppb). Within a hydrothermal mound at the Central Site, the gold concentrations are very low (12–19 ppb). Gold is concentrated in low-temperature silica-rich crusts on the massive sulfide deposit (samples 2253–1–4 and 2253–1–4a), in sulfide talus and at the contact between altered sediment and inactive chimneys (samples 2255–3–2 and 2255–3–2a). Gold is strongly depleted, and concentrations are lowest, in the massive sulfide at depth (Franklin, unpubl. data); levels also are lower in the inactive barite-enriched chimney than in the altered sediment at its base, and lower in the core of massive sulfide samples than in the crust of the same samples.

Altered muds adjacent to the mound contain significant TiO_2 and Zr. The barite crusts also contain significant TiO_2 and measureable Zr, reflecting their growth through the replacement of sediments that surround the active mounds. In contrast, the active chimneys in the AAV and the sulfide outcrop at Bent Hill contain no TiO_2 and less than 5 ppm Zr. The low TiO_2 and Zr content of the sulfide outcrop at Bent Hill suggests that this material did not form by the replacement of the surrounding sediment.

The bulk Sr concentrations in hydrothermal precipitates throughout the AAV are fairly uniform (1300–3300 ppm Sr), whereas Ba concentrations and Sr/Ba ratios vary by several orders of magnitude. The bulk Sr/Ba value of active chimneys in the AAV is more than 100 times greater than in the inactive chimneys or barite-rich crusts, which reflects the absence of barite and the high Sr contents of anhydrite in the active vents. Bulk Sr/Ba ratios in barite-rich sulfides from Bent Hill also are much lower than in active vents from the AAV.

Discussion

Fault control on the deposits

The importance of fault control on the localization of massive sulfide deposits is well documented in both modern deposits [Gorda Ridge: Rona & Clague (1989); Axial Seamount: Chase *et al.* 1985)] and in ancient deposits, where three-dimensional relationships can be determined. Kuroko-type deposits (Scott

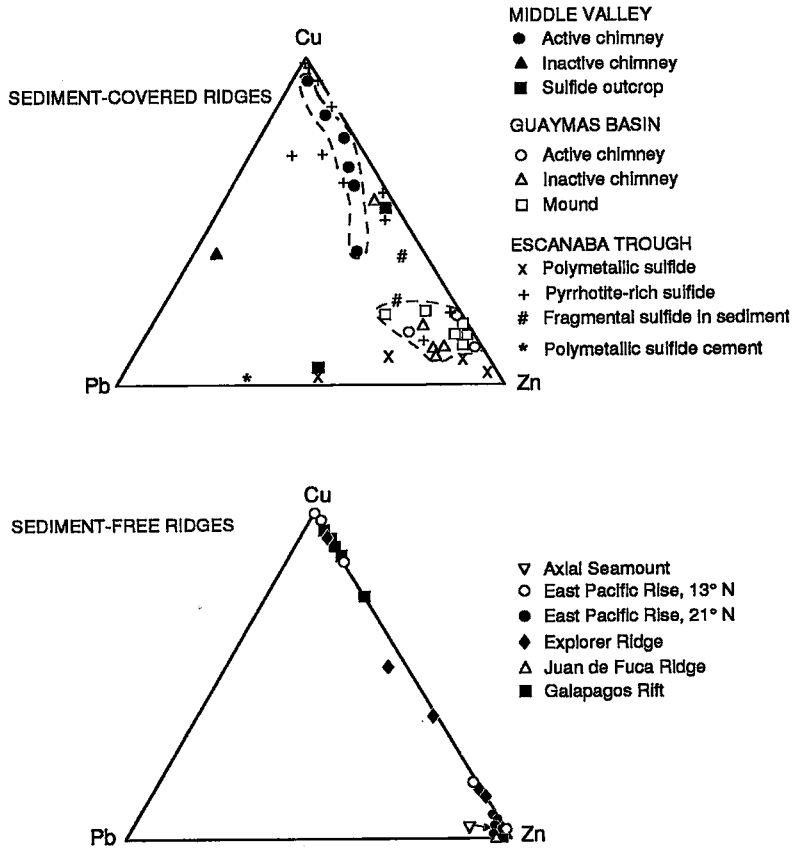

FIG. 11. Cu–Pb–Zn diagram showing modern sediment-hosted massive sulfide deposits and massive sulfide deposits on sediment-free ridges. Fields are marked for Middle Valley active chimneys and most Guaymas Basin samples. Data sources for the sedimented ridges: 1) Guaymas Basin (Peter 1986); 2) Escanaba Trough (Koski *et al.*, in press). Data sources for the bare ridges are): 1) Axial Seamount (Hannington 1986), 2) EPR, 13°N (Fouquet *et al.* 1988), 3) EPR, 21°N (Bischoff *et al.* 1983), 4) Explorer Ridge (Hannington 1986), 5) Juan de Fuca Ridge (Bischoff *et al.* 1983), 6) Galapagos (Embley *et al.* 1988).

1978, 1980) and Cyprus deposits (Adamides 1980, Constantinou 1980) occur at the intersection of orthogonal sets of fractures. The importance of syn-volcanic faults in controlling the location of base metal deposits has also been emphasized in the Canadian Shield, *e.g.*, in the Sturgeon Lake caldera (Morton *et al.* 1990), the Noranda Camp (Gibson & Watkinson 1990, Knuckey *et al.* 1982) and the Snow Lake massive sulfide deposits (Galley *et al.* 1990).

Clear fault-structures are associated with the AAV and Bent Hill areas (Fig. 2). These deposits are localized at apparent offsets in the trace of the faults, which may be a setting analogous to the orthogonal sets of fractures, although no cross structures have been defined. The fault that extends to the south of the southwestern corner of the acoustic anomaly associated with the AAV area (Fig. 2) was intersected in ODP hole 857D. This fault has exceptional permeability (down-flow rates of up to 10,000 liters per minute were measured), thus providing an adequate structure for transporting hydrothermal fluid. However, the AAV site also is coincident with a buried volcanic edifice that appears from drilling (site 858) and seismic data to be a seamount-like structure, perched on the paleo-edge of the deepest part of the Middle Valley structure. This buried seamount is a natural barrier to stratal permeability, providing an impediment to lateral movement of fluid that is trapped in the turbidite-rich lower sedimentary section at Middle Valley. Laterally moving fluids are forced

up along the margins and continue their ascent from its peak. Hydrothermal fluids ascend to the seafloor through a combination of faults and diffusional upflow through the sediments, as indicated by pore-water compositions (Lydon *et al.* 1990).

Growth of the mounds and chimneys

The surficial hydrothermal mounds in the AAV grow through inflation by precipitation of hydrothermal and alteration minerals, through mixing of hydrothermal fluid and seawater, and from trapped, conductively cooled hydrothermal fluid beneath an impermeable cap of anhydrite. Large, angular slabs of sediment on the edge of the mounds indicate that mound growth displaced, as well as replaced, the sediments.

Preliminary analysis of heat-flow data obtained along a systematic ALVIN traverse from the eastern edge of the acoustic reflector due west toward Dead Dog Mound, with a one-meter temperature probe, indicates that the highest temperatures (18°C) are found away from the mound, and cooler temperatures prevail as the active vent site is approached (8°C at the base of the mound; P. Johnson, pers. comm.). This finding suggests that mounds are self-sealing as a result of the formation of an anhydrite cap, hydrothermal precipitates and the alteration of the sediments. Penetration of seawater into the top of the mound contributes to the formation of anhydrite, Mg-rich smectite (saponite) and serpentine-group minerals in the outer crust (Percival & Ames 1993, Turner *et al.* 1991, 1993). The original pore-space in the sediment on the flanks of the mound have been infilled by lower-temperature secondary minerals such as amorphous silica, saponite, barite, marcasite and galena. The saponite casts of anhydrite observed in the mounds remain after dissolution of anhydrite. Thus, the upper layer of the mound may become sealed, thereby inhibiting the ingress of cold seawater and possibly trapping hydrothermal fluid beneath.

The presently active chimneys and vent fluids (Lydon *et al.* 1992) have low metal contents; however, the mounds below contain significant levels of base metals (Turner *et al.* 1993). This finding suggests possible depletion of the vent fluids by subseafloor precipitation. Fluid inclusions measured in anhydrite from the active vent at Bent Hill give temperatures of homogenization (265°C) that correlate with measured temperatures of the vent solutions (264°C) (Leitch 1991), as is common in many active sulfate-rich vents (Kusakabe *et al.* 1982, LeBel & Oudin 1982). The lack of abundant sulfide minerals in the active chimneys indicates that the chimneys formed primarily by quenching in seawater of moderate-temperature hydrothermal fluid with a low metal content. Seawater entrainment resulted in the formation of abundant saponite forming the inner wall of the chimneys.

The active chimneys are barium-poor, whereas the inactive chimneys and crusts at Middle Valley are barium-rich. Similar observations have been made at many areas of venting, including Axial Seamount, where lower-temperature vents are barite-rich (Feely *et al.* 1990). In the inactive barite-rich chimneys at Middle Valley, temperatures of homogenization are 170°C in primary inclusions in barite and 110°C in secondary hydrocarbon-rich inclusions (Leitch 1991). In high-temperature vent systems, barite remains in solution, and crystallizes in the water column (Feely *et al.* 1990). However, barite accumulates in lower-temperature systems typical of the waning stages of chimney growth.

Hydrothermal sediment and precipitates in the Central Site mound formed as a result of collapse of active chimneys, remobilization of constituents within the insulated mound, and direct precipitation from the hydrothermal fluid. Textural features such as corroded galena and pyrite, zoned sphalerite and recrystallized sulfides suggest that dissolution, remobilization and precipitation of the metals are important processes in the formation of mounds. Erosional processes, such as mass wasting of the chimneys, also are an important part of the development of the mounds. Turner *et al.* (1993) clearly documented chimney fragments in the mound talus. Bacterial mats on the mounds may provide a reducing sulfur-rich substrate, which favors the precipitation of metal sulfides (Jonasson & Walker 1987). The presence of bacterial mats also might aid in the development of the constructional mounds.

Implications of the sulfide assemblages and mineral compositions

In general, the variety and nature of sulfide assemblages from Middle Valley resemble those associated with hydrothermal activity in sediment-hosted vent fields at Escanaba Trough and at Guaymas Basin (Koski *et al.* 1988, Peter & Scott 1988). Observations at Bent Hill suggest that the mineralization here most closely resembles the sulfide deposits at Escanaba Trough, where massive sulfides outcrop along the margins of several uplifted sediment-capped hills. The sulfides at Escanaba consist of massive pyrite–pyrrhotite assemblages, together with low-temperature polymetallic sulfide and barite crusts. Limited, active venting at temperatures less than 220°C occurs from sulfide chimneys on the massive sulfide mounds (Koski *et al.* 1988, Koski *et al.*, in press). Mineralization in the AAV is most similar to that due to the presently active hydrothermal vents in the Guaymas Basin. Mineralization is hosted at both sites in sulfate-dominant chimneys that vent greyish, moderate-temperature fluids and contain only minor sulfides (*e.g.*, Koski *et al.* 1985, Peter & Scott 1988).

Three distinct mineral assemblages are present at Middle Valley. In the AAV, moderate-temperature

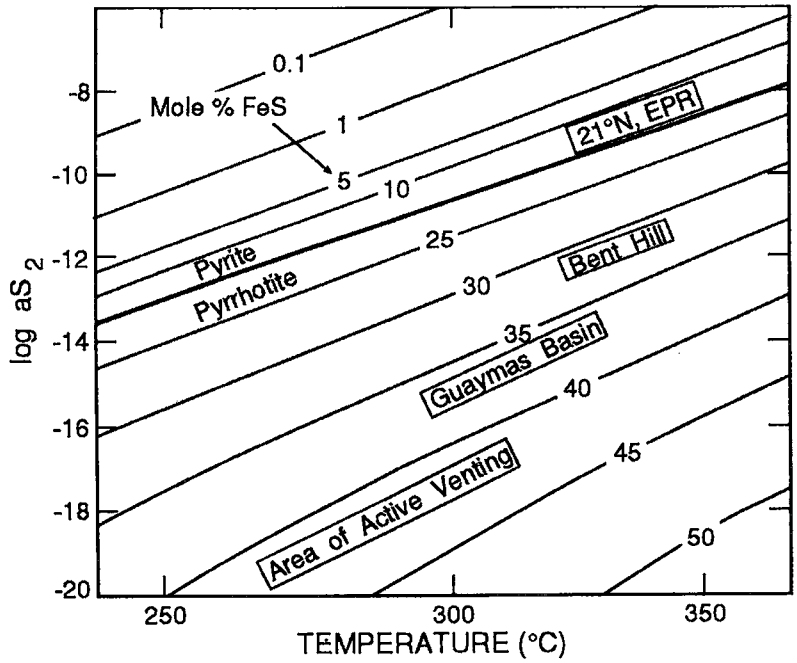

FIG. 12. T–$a(S_2)$ diagram showing the relative compositions of sphalerite in hydrothermal precipitates from Middle Valley (Area of Active Venting, Bent Hill), Guaymas Basin, and 21°N, East Pacific Rise. Average mole % FeS contents only are shown; data are from Zierenberg *et al.* (1984), Peter & Scott (1988), and this study. Contours of mole % FeS are based on data from Toulmin & Barton (1964), Scott & Barnes (1971), and Czamanske (1974). Sphalerite from the Area of Active Venting and Guaymas Basin formed at low $a(S_2)$ conditions; sphalerite from Bent Hill and the Escanaba Trough formed at intermediate values of $a(S_2)$, close to the pyrite–pyrrhotite boundary.

(276°C) active vents are composed of an anhydrite–smectite assemblage in which pyrrhotite is the dominant sulfide phase. Lower-temperature vents, inactive chimneys, and hydrothermal crusts consist dominantly of barite, amorphous silica, and clays, with pyrite and pyrrhotite present in varying amounts. The inactive chimneys are notable for the presence of abundant bitumen. The sulfide deposits in the Bent Hill area comprise a pyrite–pyrrhotite assemblage with abundant copper- and zinc-bearing phases. These relations reflect a wide range of fluid compositions, from relatively high-temperature (*ca.* ≥300°C), metal-rich and sulfur-bearing fluids that formed the sulfide deposits in the Bent Hill area to lower-temperature (<300°C), metal-depleted and sulfur-poor fluids that are currently venting from chimneys in the AAV. The active vents in the AAV appear to tap fluids derived from the low-temperature interaction of seawater with the sediment fill in Middle Valley. They have a characteristically high pH (5.1–5.8) and are locally charged with bitumens derived from the thermal cracking of organic carbon in the sediments. In contrast, the massive sulfides at Bent Hill appear to be the product of either an earlier stage of the present hydrothermal event related to high-temperature interaction of circulating seawater with basaltic crust in the basement, or a completely different, unrelated hydrothermal system.

The broad range of FeS contents in sphalerite from the Middle Valley sulfides (8–60 mole % FeS) reflects the wide range of conditions of sulfide precipitation. The presence of high-iron sphalerite from chimneys in the AAV suggests a fluid composition buffered to low $a(S_2)$ (*i.e.*, in equilibrium with pyrrhotite: Fig 12). Although no sphalerite data exist for the inactive chimneys, the presence of abundant hydrocarbons (bitumen) also attests to a low $a(O_2)$ and $a(S_2)$ in the fluids. Similar conditions of precipitation are suggested by the composition of sphalerite from deposits in other sedimented environments (*e.g.*, 22–55 mole % FeS in Guaymas Basin chimneys: Peter & Scott 1988). Sphalerite from these deposits typically is more iron-rich than sphalerite from bare-ridge deposits. For example, the sphalerite recovered from sites at

Explorer Ridge and Axial Seamount on the Juan de Fuca Ridge and from TAG and Snakepit on the Mid-Atlantic Ridge contains less than 30 and usually less than 10 mole % FeS (Hannington *et al.* 1991). The most Fe-rich compositions of sphalerite in bare-ridge deposits are associated with high-temperature fluids in pyrrhotite-rich black smoker chimneys (*e.g.*, 21°N, EPR: Fig. 12). The high iron contents in sphalerite from the AAV at Middle Valley and the Guaymas Basin reflect the strong buffering of fluid compositions [*e.g.*, low $a(O_2)$, low $a(S_2)$, and low Fe and S concentrations] by local interaction with organic-matter-rich sediments. Pb and Sr isotopic data also indicate a strong component of a sedimentary source component (Goodfellow & Franklin, in press). The iron contents of sphalerite from the southern Bent Hill massive sulfide deposit are much lower than those from the AAV active chimneys, reflecting precipitation from a fluid with a significantly higher $a(S_2)$ (*i.e.*, close to pyrite–pyrrhotite). Sphalerite from sulfide deposits at Bent Hill, is similar in composition to sphalerite from Escanaba Trough (averaging close to 27 mole % FeS: Hoyt 1992), which suggests a fluid source intermediate between sediments and basalt.

Similar trends are observed for the compositions of pyrrhotite from different deposits. Pyrrhotite compositions ranging from 48.3 to 50.0 at.% Fe were found in the pyrrhotite ± sphalerite ± isocubanite assemblages from moderate-temperature chimneys at Dead Dog Mound (AAV). These compositions indicate a low $a(S_2)$ (*e.g.*, Toulmin & Barton 1964) and are consistent with the high iron content of coexisting sphalerite (Fig. 12). Pyrrhotite compositions in both sulfide outcrops at Bent Hill range from 47.3 to 47.9 at.% Fe and are consistent with a higher $a(S_2)$. Similar compositions of pyrrhotite were found in massive sulfide from the Escanaba Trough deposits (averaging 47.3 at.% Fe: Hoyt 1992).

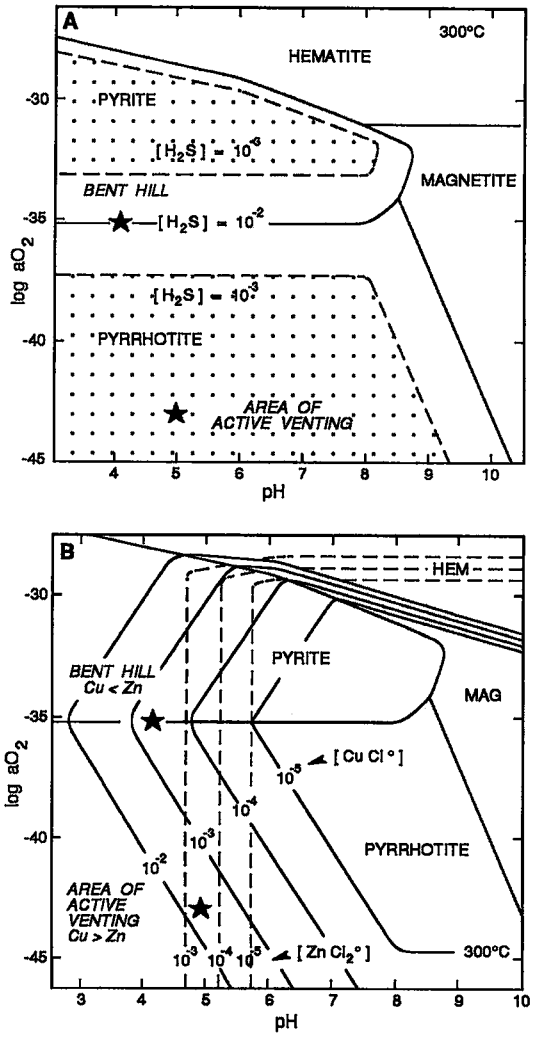

FIG. 13. A. pH–$a(O_2)$ diagram showing the fields of stability for the principal Fe-sulfides and oxides at 300°C and total reduced sulfur concentrations of 10^{-2} M and 10^{-3} M H_2S. Sulfides from Bent Hill comprise a dominantly pyrite–pyrrhotite assemblage that formed at relatively high $a(O_2)$ from sulfur-rich hydrothermal fluids. Active chimneys in the AAV formed at low $a(O_2)$ and contain pyrrhotite as the dominant Fe-sulfide. At low concentrations of total sulfur (*e.g.*, 10^{-3} M H_2S), the stability fields of the principal Fe-sulfides collapse, and magnetite will form at the expense of pyrite and pyrrhotite. Drilling beneath the Bent Hill deposits suggests that massive sulfides at depth have been affected by a recent flux of low-sulfur fluids similar to those presently venting in the AAV. This has resulted in significant recrystallization of the sulfides and replacement by late-stage magnetite. Equilibrium constants are calculated from Barton (1984) and Bowers *et al.* (1984). B. The solubility of chalcopyrite [CuCl°] and sphalerite [$ZnCl_2$°] as a function of pH and $a(O_2)$ at 300°C and 10^{-2} M H_2S. The solubility of chalcopyrite at low $a(O_2)$ is significantly greater than that of sphalerite in the same solutions, suggesting that vent fluids in the AAV may be enriched in copper relative to zinc. Such fluids may effectively leach copper from subsurface sediments. This could account for the depletion in copper in subseafloor sediments in the AAV (see Fig. 14). Equilibrium constants are calculated from Barton (1984), Bowers *et al.* (1984), Crerar & Barnes (1976), and Ruaya & Seward (1986).

The mineralogical data suggest that massive sulfides at Bent Hill formed from hydrothermal fluids similar to those currently venting in the Escanaba Trough. Total concentrations of dissolved sulfur were likely between 10^{-2} and 10^{-3} M H_2S, and seem to have been intermediate between bare-ridge hydrothermal fluids, like those at 21°N EPR, and the fluids associated with hydrothermal activity in the Guaymas Basin (*e.g.*, Campbell *et al.* 1992). Vent fluids responsible for mineralization at Bent Hill would have plotted close to the pyrite–pyrrhotite boundary in pH–$a(O_2)$ space (Figs. 13A, B). In contrast, sphalerite compositions for the active chimneys in the AAV indicate equilibration at low $a(O_2)$ and $a(S_2)$, and fluids responsible for present-day mineralization in the AAV plot well within the pyrrhotite field.

Recent drilling at Site 856 during Leg 139 of the ODP intersected 95 m of massive sulfide beneath the Bent Hill deposit. This deposit is presumed to have formed at the same time as the sulfide outcrop below the active chimney at Bent Hill, owing to the similar textural, mineralogical and geochemical characteristics of the massive sulfide deposits. However, the sulfides in Hole 856G comprise zones of pyrite, pyrrhotite and a mixed pyrite–pyrrhotite assemblage that has undergone significant recrystallization and late-stage replacement of sulfides by magnetite (Davis *et al.* 1992). The growth of magnetite from pyrite and pyrrhotite reflects the re-equilibration of the sulfides with a late-stage, sulfur-poor fluid similar to that currently venting in the AAV. At low concentrations of total sulfur (*e.g.*, 10^{-3} M H_2S), the stability fields for the principal Fe-sulfides will diminish, and magnetite will begin to form at the expense of pyrite and pyrrhotite (*e.g.*, Fig. 13A).

Implications of data on bulk compositions

Base metal contents in the Middle Valley sulfides are low in the active chimneys, as are the Zn/Cu and Zn/Pb ratios (generally <1 and <10, respectively). The lack of base metals in the AAV is likely due to the very low initial contents of base metals in the hydrothermal fluids. At the observed temperature and high pH of active vents in the AAV, the solubility of all base metals is low (Franklin *et al.* 1981), and no major subseafloor accumulation of metals was encountered beneath the AAV during drilling at site 858 (Davis *et al.* 1992). As well, pore fluids recovered from Site 857 (Fig. 2) at depths in excess of 425 m are very similar in major-element composition to the actively venting fluids in the AAV site (Davis *et al.* 1992). These fluids are in equilibrium with their host clastic and hemipelagic sedimentary rocks and may represent metamorphic fluids.

Examination of the trace-element geochemistry of sediments (Davis *et al.* 1992) in the Site 857 drill holes, south of the AAV, shows that copper is virtually absent from the rocks in equilibrium with the vent-type pore fluids at depth, whereas zinc is only slightly depleted (Fig. 14). This finding indicates that the hydrothermal fluids, although metal-depleted overall, may carry significantly more copper than zinc. This is supported by the unusually low Zn/Cu ratio of precipitates in the active chimneys. Figure 13B shows that the solubility of chalcopyrite in fluids from the AAV may be more than an order of magnitude greater than that of sphalerite. Thus selective leaching of trace metals from the sediments at site 857, south of the AAV, could account for the significant depletion of copper relative to zinc (Fig. 14).

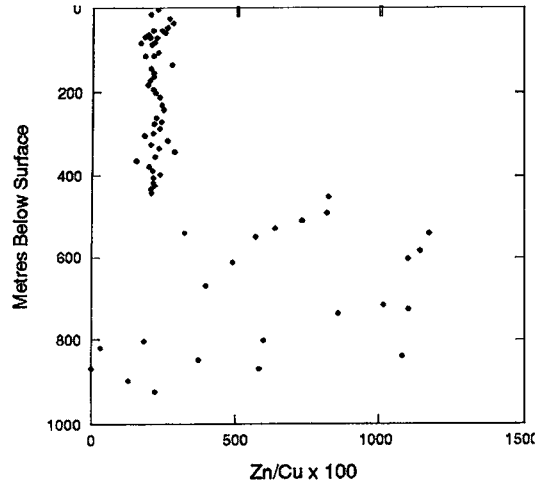

FIG. 14. The variation in Zn/Cu ratio with depth in hemipelagic sediment from ODP Site 857 illustrates a significant depletion of copper below 430 m. Actively venting chimneys at the AAV are copper-rich (relative to levels of zinc).

If compared to ancient massive sulfide deposits (see Franklin *et al.* 1981), the sulfide portion of the active chimneys from Middle Valley places them in the Zn–Pb–Cu group of deposits, more typical of felsic- or sediment-dominated terranes. Some important information regarding the distribution of base and precious metals is evident on examination of a correlation matrix for the data from the active chimneys. Silver is correlated with lead (0.99) and barium (0.84), but not with copper (0.48). Franklin *et al.* (1981) showed that in zinc–copper deposits, silver is strongly correlated with copper, but in Zn–Pb–Cu deposits, it correlates with Pb. Samples from the active vents thus seem to be much more similar to the latter class of volcanogenic massive sulfide deposit. The close correlation of silver with barium may indicate that silver has remained conservative in the vent fluids, and has coprecipitated with barite and galena in the relatively low-temperature parts of the chimneys. The high uniform Sr contents of hydrothermal precipitates at

Middle Valley reflects a large contribution of sediment-derived Sr, possibly from dissolution of carbonate in planktonic foraminifera and carbonate nodules during hydrothermal venting. These data are consistent with Pb and Sr isotopic data (Goodfellow & Franklin, in press), which indicates that the fluids responsible for these active vents have probably equilibrated with sedimentary material.

In contrast to the active chimneys, the Bent Hill massive sulfide deposits have high Zn/Cu and Zn/Pb ratios, at surface (2253–1–3, Table 9) and at depth (Davis *et al.* 1992). Although trace amounts of galena and Pb–Sb–As sulfosalts occur on the outer upper edge of the massive sulfide deposit, these mineral phases are volumetrically insignificant. The massive sulfide deposits at Bent Hill lie in the Zn–Cu group of deposits as defined by Franklin *et al.* (1981). The base metal content reflects predominantly basaltic source-rocks for the massive sulfide deposits. Strontium isotopic data, intermediate between a value typical of mid-ocean-ridge basalts and hemipelagic sediments, reflect both basaltic and sedimentary reservoirs for the hydrothermal fluid that formed the sulfides at Bent Hill (Goodfellow *et al.* 1990).

Remobilization, dissolution and reprecipitation of both base and precious metals in the sulfide deposit are evident in the observed textures, the presence of galena, gold and Pb–Sb–As sulfosalts concentrated on the upper fringe of the deposit and the lack of these minerals at depth (Davis *et al.* 1992), and variations in base metal ratios at depth (Davis *et al.* 1992). These all indicate a metal zonation typical of many ancient massive sulfide deposits (Franklin *et al.* 1982, Knuckey *et al.* 1982). Late-stage hydrothermal fluids remobilized and redistributed metals in the massive sulfide deposit at Bent Hill.

Conclusions

Our studies indicate that, at Middle Valley, two completely different types of deposit are defined by their contrasting assemblages of minerals, geochemistry and source compositions. Mineralization at the AAV and in the active vent at Bent Hill is sulfur-poor and formed from fluids indicative of seawater–sediment interaction. The older sulfide deposits at Bent Hill formed from fluids with a higher $a(S_2)$ and $a(O_2)$ and a much greater degree of fluid–basalt interaction.

Indicators of a significant contribution of sedimentary material to the venting hydrothermal fluids are: low total levels of base metals and high levels of Pb compared to bare-ridge deposits, a bulk enrichment in Sr, a characteristic pyrrhotite-dominant sulfide assemblage, Pb and Sr isotopic data (Goodfellow & Franklin, in press), high-pH fluids with low $a(S_2)$ and low $a(O_2)$ based on mineral chemistry and associated assemblages, and the selective leaching of copper from the sediment below site 857.

Indicators of a significant basaltic component to the hydrothermal fluid that precipitated the Bent Hill massive sulfide deposits includes: high copper and zinc content, low Pb and Sr isotopic values (Goodfellow & Franklin, in press), and abundant primary pyrite + pyrrhotite. Late-stage hydrothermal fluids have affected the original sulfide assemblage at Bent Hill, as indicated by the recrystallization of sulfides, the formation of magnetite beneath Bent Hill, and the dissolution of zinc and gold from the ODP sulfides at depth (Davis *et al.* 1992) and precipitation near the mound surface, resulting in a zone-refined deposit typical of many ancient deposits on land (Franklin *et al.* 1981, Knuckey *et al.* 1982, Sangster 1972).

The two hydrothermal events, represented by the active vents (AAV and Bent Hill) and the massive sulfide deposits at Bent Hill, may represent a continuum process of crustal cooling within a recently active rift environment or two independent events with a coincidental spatial relationship.

Acknowledgements

The authors thank 1) the ATLANTIS II and DSRV ALVIN crews for their efforts and help in obtaining the samples, and 2) the scientists, M. Black, W. Goodfellow, P. Johnson, K. Juniper, R. McDuff, E. Southward, B. Taylor and R. Zierenberg. This contribution benefitted from the efforts of many staff at the GSC: L.K. Radburn provided excellent SEM microphotographs, G.D. Pringle wrote computer programs to calculate mineral formulae, J.A.R. Stirling gave excellent advice for the analysis of such fine-grained material by electron microprobe. We are particularly grateful to R. Lancaster and K. Nyguen for their drafting expertise. R. Koski, I.R. Jonasson and M. Zientek clarified many aspects of the manuscript in their careful reviews.

References

Adamides, (1980): The form and environment of formation of the Kalavasos ore deposits, Cyprus. *In* Ophiolites: Int. Ophiolite Symp. Proc. (Cyprus, 1977; A. Panayiotou, ed.). *Cyprus Ministry Agriculture Nat. Resources, Geol. Survey Dep.*, 117-178.

Barton, P.B., Jr. (1984): Redox reactions in hydrothermal fluids. *In* Fluid–Mineral Equilibria in Hydrothermal Systems (R.W. Henley, A.H. Truesdell & P.B. Barton, Jr., eds.). Rev. Econ. Geol. **1**, 99-114.

Bischoff, J.L., Rosenbauer, R.J., Aruscavage, P.J., Baedecker, P.A. & Crock, J.G. (1983): Seafloor massive sulfide deposits from 21°N, East Pacific Rise; Juan de Fuca Ridge; and Galapagos Rift: bulk chemical composition and economic implications. *Econ. Geol.* **78**, 1711-1720.

Bowers, T.S., Jackson, K.J. & Helgeson, H.C. (1984):

Equilibrium Activity Diagrams for Coexisting Minerals and Aqueous Solutions at Pressures and Temperatures to 5 kb and 600°C. Springer-Verlag, New York.

CAMPBELL, A.C., GERMAN, C.R., PALMER, M.R. & EDMOND, J.M. (1992): Chemistry of hydrothermal fluids from the Escanaba Trough, Gorda Ridge. *U.S. Geol. Surv., Bull.* (in press).

CHASE, R.L., DELANEY, J.R., KARSTEN, J.L., JOHNSON, H.P., JUNIPER, S.K., LUPTON, J.E., SCOTT, S.D., TUNNICLIFFE, V., HAMMOND, S.R. & MCDUFF, R.E. (CASM Research Group) (1985): Hydrothermal vents on an axis seamount of the Juan de Fuca Ridge. *Nature* **317**, 212-214.

CONSTANTINOU, G. (1980): Metallogenesis associated with the Troodos ophiolite. *In* Ophiolites: Int. Ophiolite Symp. Proc. (Cyprus, 1977; A. Panayiotou, ed.). *Cyprus Ministry Apriculture Nat. Resources, Geol. Survey Dep.*, 663-674.

CRERAR, D.A. & BARNES, H.L. (1976): Ore solution chemistry. V. Solubilities of chalcopyrite and chalcocite assemblages in hydrothermal solutions at 200 to 350°C. *Econ. Geol.* **71**, 772-794.

CURRIE, R.G, DAVIS, E.E., RIDDIHOUGH, R.P. & SAWYER, B.S. (1985): Juan de Fuca Ridge Atlas): preliminary Seabeam bathymetry, *Geol. Surv. Can., Open-File Rep.* **1143**.

CZAMANSKE, G.K. (1974): The FeS content of sphalerite along the chalcopyrite – pyrite – bornite sulfur fugacity buffer. *Econ. Geol.* **69**, 1328-1334.

DAVIS, E.E., GOODFELLOW, W.D., BORNHOLD, B.D., ADSHEAD, J., BLAISE, B., VILLINGER, H. & LECHEMINANT, G.M. (1987): Massive sulfides in a sedimented rift valley, northern Juan de Fuca Ridge. *Earth Planet. Sci. Lett.* **82**, 49-61.

——— & LISTER, C.R.B. (1977): Tectonic structures on the Juan de Fuca Ridge. *Geol. Soc. Am. Bull.* **88**, 346-363.

———, MOTTL, M.J., FISHER, A.T., ET AL. (1992): Proceedings of the Ocean Drilling Program, Initial Reports 139: College Station, TX (Ocean Drilling Program), 1-1026.

DEGENS, E.T. & ROSS, D., eds. (1969): *Hot Brines and Recent Heavy Metal Deposits in the Red Sea; a Geochemical and Geological Account.* Springer, New York.

EMBLEY, R.W., JONASSON, I.R., PERFIT, M.R., FRANKLIN, J.M., TIVEY, M.A., MALAHOFF, A., SMITH, M.F. & FRANCIS, T.J.G. (1988): Submersible investigation of an extinct hydrothermal system on the Galapagos Ridge: sulfide mounds, stockwork zone and differentiated lavas. *Can. Mineral.* **26**, 517-539.

FEELY, R.A., GEISELMAN, T.L., BAKER, E.T., MASSOTH, G.J. & HAMMOND, S.R. (1990): Distribution and composition of hydrothermal plume particles from the ASHES Vent Field at Axial Volcano, Juan de Fuca Ridge. *J. Geophys. Res.* **95**, 12,855-12,873.

FOUQUET, Y., AUCLAIR, G., CAMBON, P. & ETOUBLEAU, J. (1988): Geological setting and mineralogical and geochemical investigations on sulfide deposits near 13°N on the East Pacific Rise. *Marine Geol.* **84**, 145-178.

FRANKLIN, J.M., GOODFELLOW, W.D., AMES, D.E., LYDON, J.W., JONASSON, I.R. & DAVIS, E.E. (1991): Middle Valley, a major centre of hydrothermal activity in a sedimented ridge crest, northern Juan de Fuca Ridge. *Geol. Surv. Can., Current Activities Forum (Ottawa), Program Abstr.*, 20.

———, ———, BLAISE, B., ANGLIN, C.D., HARVEY-KELLY, F.L. & MACDONALD, R. (1987): Geological map and distribution of sulfide deposits in Middle Valley, northern Juan de Fuca Ridge. *Am. Geophys. Union. Trans. (Eos)* **68**(44), 1545 (abstr.).

———, JOHNSON, H.P. & CURRIE, R. (in press): SeaMARC 1A side-scan imagery of the Middle Valley area, northern Juan de Fuca Ridge. *Geol. Surv. Can., Open File.*

———, LYDON, J.W. & SANGSTER, D. (1981): Volcanic-associated massive sulfide deposits. *Econ. Geol.*, *75th Anniv. Vol.*, 485-627.

GALLEY, A.G., BAILES, A.H., SYME, E.C., BLEEKER, W., MACEK, J.J. & GORDON, T.M. (1990): Geology and mineral deposits of the Flin Flon and Thompson belts, Manitoba. *Geol. Surv. Can., Open-File Rep.* **2165**.

GIBSON, H.L. & WATKINSON, D.H. (1990): Volcanogenic massive sulphide deposits of the Noranda cauldron and shield volcano, Quebec. *In* The Northwestern Quebec Polymetallic Belt (M. Rive, P. Verpaelst, Y. Gagnon, J.M. Lulin, G. Riverin & A. Simard, eds.). *Can. Inst. Mining Metall., Spec. Vol.* **43**, 119-132.

GOODFELLOW, W.D. & BLAISE, B. (1988): Sulfide formation and hydrothermal alteration of hemipelagic sediment in Middle Valley, northern Juan de Fuca Ridge. *Can. Mineral.*, **26**, 675-696.

——— & FRANKLIN, J.M. (1993): Geology, mineralogy and geochemistry of sediment-hosted clastic massive sulfide in shallow cores, Middle Valley, northern Juan de Fuca Ridge. *Econ. Geol.* **88** (in press).

———, ——— & LYDON, J.W. (1990): Geological setting and origin of the Middle Valley sulfide deposits, northern Juan de Fuca Ridge. Trans. Am. Geophys. Union (Eos) **71**(43), 1565 (abstr.).

HANNINGTON, M.D. (1986): *Geology, Mineralogy and Geochemistry of a Silica – Sulfate – Sulfide Deposit, Axial Seamount, NE Pacific Ocean.* M.Sc. thesis, Univ. Toronto, Toronto, Ontario.

——— & GORTON, M.P. (1991): Analysis of sulfides for gold and associated trace metals by direct neutron activation with a low-flux reactor. *Geostandards Newslett.* **15**, 145-154.

———, HERZIG, P., SCOTT, S., THOMPSON, G. & RONA, P. (1991): Comparative mineralogy and geochemistry of

gold-bearing sulfide deposits on the mid-ocean ridges. *Marine Geol.* **101**, 217-248.

——— & SCOTT, S.D. (1989): Sulfidation equilibria as guides to gold mineralization in volcanogenic massive sulfides: evidence from sulfide mineralogy and the composition of sphalerite. *Econ. Geol.* **84**, 1978-1995.

HOYT, T.L. (1992): *Mineral Chemistry of Massive Sulfide and Sulfate Samples from Escanaba Trough, Southern Gorda Ridge.* M.Sc. thesis, Univ. California, Davis, California.

JOHNSON, H.P., TIVEY, M.A. & FRANKLIN, J.M. (1990): Tectonic control on hydrothermal systems on the northern Juan de Fuca Ridge): Middle Valley and the Endeavour segment. *Trans. Am. Geophys. Union (Eos)* **71**(43), 1566 (abstr.).

JOIDES (1991): Leg 139: Sedimented Ridges. 1. Science Operator Report. *JOIDES J.* **17**(3), 8-12.

JONASSON, I.R. & WALKER, D.A. (1987): Micro-organisms and their debris as substrates for base metal sulfide nucleation and accumulation in some Mid-Ocean Ridge deposits. *Trans. Am. Geophys. Union (Eos)* **68**(44), 1546 (abstr.).

KAPPEL, E.S. & FRANKLIN, J.M. (1989): Relationships between geologic development of ridge crests and sulfide deposits in the northeast Pacific Ocean. *Econ. Geol.* **84**, 485-505.

KNUCKEY, M.J., COMBA, C.D.A. & RIVERIN, G. (1982): Structure, metal zoning and alteration at the Millenbach deposit, Noranda, Quebec. *Geol. Assoc. Can., Spec. Pap.* **25**, 255-295.

KOSKI, R.A., BENNINGER, L.M., ZIERENBERG, R.A. & JONASSON, I.R. (1993): Composition and growth history of hydrothermal deposits in Escanaba Trough, southern Gorda Ridge. *U.S. Geol. Surv., Bull.* **2022** (in press).

———, LONSDALE, P.F., SHANKS, W.C., III, BERNDT, M.E. & HOWE, S.S (1985): Mineralogy and geochemistry of a sediment-hosted hydrothermal sulfide deposit from the Southern Trough of Guaymas Basin, Gulf of California. *J. Geophys. Res.* **90**, 6695-6707.

———, SHANKS, W.C., III, BOHRSON, W.A. & OSCARSON, R.L. (1988): The composition of massive sulfide deposits from the sediment-covered floor of the Escanaba Trough, Gorda Ridge: implications for depositional processes. *Can. Mineral.* **26**, 655-673.

KUSAKABE, M., CHIBA, H. & OHMOTO, H. (1982): Stable isotopes and fluid inclusion study of anhydrite from East Pacific Rise at 21°N, *Geochem. J.* **16**, 89-95.

LE BEL, L. & OUDIN, E. (1982): Fluid inclusion studies of deep-sea hydrothermal sulfide deposits on the East Pacific Rise near 21°N. *Chem. Geol.* **37**, 129-136.

LEITCH, C.H.B. (1991): Preliminary studies of fluid inclusions in barite from the Middle Valley sulfide mounds, northern Juan de Fuca Ridge. *Geol. Surv. Can., Pap.* **91-1A**, 27-30.

LONSDALE, P.F., BISCHOFF, J.L., BURNS, V.M., KASTNER, M. & SWEENEY, R.E. (1980): A high-temperature hydrothermal deposit on the seabed at a Gulf of California spreading center. *Earth Planet. Sci. Lett.* **49**, 8-20.

LYDON, J.W., GOODFELLOW, W.D. & AMES, D.E. (1990): Composition of subsurface hydrothermal plumes, Middle Valley, northern Juan de Fuca Ridge. *Eighth IAGOD Meet., Program Abstr.*, A273.

———, ——— & GRÉGOIRE, D.C. (1992): Chemical composition of vent and pore fluids in an active hydrothermal discharge zone, Middle Valley. *Geol. Surv. Can., Minerals Colloquium (Ottawa), Program Abstr.*, 24.

MORTON, J.L., HOLMES, M.L. & KOSKI, R.A. (1987): Volcanism and massive sulfide formation at a sedimented spreading center, Escanaba Trough, Gorda Ridge, northeast Pacific Ocean. *Geophys. Res. Lett.* **14**, 769-772.

———, KOSKI, R.A., NORMARK, W.R. & ROSS, S.L. (1990): Distribution and composition of massive sulfide deposits at Escanaba Trough, southern Gorda Ridge. *In* Gorda Ridge: a Seafloor Spreading Center in the United States' Exclusive Economic Zone (G.R. McMurray, ed.). Springer-Verlag, New York (77-92).

PERCIVAL, J.P. & AMES, D.E. (1993): Clay mineralogy of active hydrothermal chimneys and associated mounds, Middle Valley, northern Juan de Fuca Ridge. *Can. Mineral.* **31**, 957-971.

PETER, J.M. (1986): *Genesis of Hydrothermal Vent Deposits in the Southern Trough of Guaymas Basin, Gulf of California: a Mineralogical and Geochemical Study.* M.Sc. thesis, Univ. Toronto, Toronto, Ontario.

——— & SCOTT, S.D. (1988): Mineralogy, composition, and fluid-inclusion microthermometry of seafloor hydrothermal deposits in the southern trough of Guaymas Basin, Gulf of California. *Can. Mineral.* **26**, 567-587.

RONA, P.A. & CLAGUE, D.A. (1989): Geologic controls of hydrothermal discharge on the northern Gorda Ridge. *Geology* **17**, 1097-1101.

RUAYA, J.R. & SEWARD, T.M. (1986): The stability of chlorozinc (II) complexes in hydrothermal solutions up to 350°C. *Geochim. Cosmochim. Acta* **50**, 651-661.

SANGSTER, D.F. (1972): Precambrian volcanogenic massive sulphide deposits in Canada: a review. *Geol. Surv. Can., Pap.* **72-22.**

SCOTT, S.D. (1978): Structural control of the Kuroko deposits of the Hokuroko district, Japan. *Min. Geol.* **28**, 301-311.

——— (1980): Geology and structural control of Kuroko-type massive sulphide deposits. *Geol. Assoc. Can., Spec. Pap.* **70**, 705-722.

——— (1983): Chemical behaviour of sphalerite and arsenopyrite in hydrothermal and metamorphic environments. *Mineral. Mag.* **47**, 427-435.

——— & BARNES, H.L. (1971): Sphalerite geothermometry and geobarometry. *Econ. Geol.* **66**, 653-669.

SIMONEIT, B.R.T., GOODFELLOW, W.D. & FRANKLIN, J.M. (1992): Hydrothermal petroleum at the seafloor and organic matter alteration in sediments of Middle Valley, northern Juan de Fuca Ridge. *Appl. Geochem.* **7**, 257-264.

STAKES, D.S., FRANKLIN, J.M. & THE LEG 139 SHIPBOARD SCIENTIFIC PARTY (1991): Initial results from drilling in the Middle Valley of the Juan de Fuca Ridge: hydrothermal alteration of mafic sills in a sedimented ridge environment. *Trans. Am. Geophys. Union (Eos)* **72**(44), 553 (abstr.).

TOULMIN, P., III & BARTON, P.B., JR. (1964): A thermodynamic study of pyrite and pyrrhotite. *Geochim. Cosmochim. Acta* **28**, 641-671.

TURNER, R.J.W., AMES, D.E., FRANKLIN, J.M., GOODFELLOW, W.D., LEITCH, C.H.B. & HOY, T. (1993): Character of active hydrothermal mounds and nearby altered hemipelagic sediments in the hydrothermal areas of Middle Valley, northern Juan de Fuca Ridge: shallow core data. *Can. Mineral.* **31**, 973-995.

———, LEITCH, C.H.B, AMES, D.E., HOY, T., FRANKLIN, J.M. & GOODFELLOW, W.D. (1991): Character of hydrothermal mounds and adjacent altered sediments, active hydrothermal areas, Middle Valley sedimented rift, northern Juan de Fuca Ridge, northeastern Pacific : evidence from ALVIN push cores. *Geol. Surv. Can., Pap.* **91-1E**, 99-108.

VON DAMM, K.L. & BISCHOFF, J.L. (1987): Chemistry of hydrothermal solutions from the southern Juan de Fuca Ridge. *J. Geophys. Res.* **92**, 11,334-11,346.

ZIERENBERG, R.A., SHANKS, W.C., III & BISCHOFF, J.L. (1984): Massive sulfide deposits at 21°N, East Pacific Rise: chemical composition, stable isotopes, and phase equilibria. *Geol. Soc. Am. Bull.* **95**, 922-929.

Received August 7, 1992, revised manuscript accepted March 5, 1993.